

Stereochemical and Conformational Control of Metal Redox Processes: The Co-ordination Chemistry of the Mixed N- and S-Donor Macrocyclic Crowns [18]aneN₂S₄ and Me₂[18]aneN₂S₄

By Gillian Reid and Martin Schroder

DEPARTMENT OF CHEMISTRY, UNIVERSITY OF EDINBURGH,
WEST MAINS ROAD, EDINBURGH EH9 3JJ

1 Introduction

Although thioethers are generally regarded as very poor ligands to transition metal centres,¹ recent studies have established that macrocyclic thioethers readily bind to certain metal ions to form highly stable complexes.^{2–4} The enhanced thermodynamic and kinetic stability of these cyclic complexes can be attributed to the macrocyclic effect.⁵ The chemistry of cyclic polythioether crowns with late transition metal ions (particularly those of the second and third rows) therefore complements the well-established co-ordination chemistry of Group I and II metal ions with polyoxo crown ethers.^{6–8} Transition metal macrocyclic co-ordination chemistry is dominated however by complexation of polyaza ligands such as porphyrins, phthalocyanines, and their synthetic analogues.^{6,8} Saturated polyaza ligands such as cyclam, [14]aneN₄, are generally considered to act only as σ -donors to metal centres; for softer thioether S-donor ligands, however, π -effects may be important.⁹

Although the factors influencing the stability of homoleptic metal macrocyclic complexes are now quite well established,^{6–8,10,11} fewer coherent, systematic studies of the co-ordination chemistry of mixed donor macrocyclic species have been undertaken. As part of a study on the selective complexation of transition metal ions by polydentate ligands, including mixed-donor macrocycles, Lindoy, Tasker, and co-workers have reported^{11,12} a series of elegant studies on

¹ S G Murray and F R Hartley, *Chem. Rev.*, 1981, **81**, 365

² A J Blake and M Schroder, *Adv. Inorg. Chem.*, 1990, **35**, 1

³ M Schroder, *Pure Appl. Chem.*, 1988, **60**, 517

⁴ S R Cooper, *Acc. Chem. Res.*, 1988, **21**, 141

⁵ R D Hancock and A E Martell, *Comments Inorg. Chem.*, 1988, **6**, 237

⁶ L F Lindoy, 'The Chemistry of Macrocyclic Ligand Complexes', Cambridge University Press, Cambridge, 1989

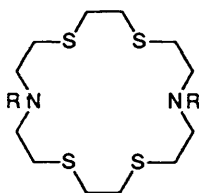
⁷ 'Coordination Chemistry of Macrocyclic Compounds', ed G A Melson. Plenum Press, New York, 1979

⁸ 'Host Guest Complex Chemistry: Macrocycles', ed F Vogtle and E Weber, Springer Verlag, Berlin 1985

⁹ A J Blake, A J Holder, T I Hyde, and M Schroder, *J. Chem. Soc., Chem. Commun.*, 1989, 1433.

¹⁰ D H Busch, *Acc. Chem. Res.*, 1978, **11**, 392

¹¹ K Henrick, P A Tasker, and L F Lindoy, *Prog. Inorg. Chem.*, 1985, **33**, 1, K Henrick, L F Lindoy, M McPartlin, P A Tasker, and M P Wood, *J. Am. Chem. Soc.*, 1984, **106**, 1641.



[18]aneN₂S₄: R = H
 Me₂[18]aneN₂S₄: R = Me

the effects of systematic ligand variation on metal binding and stereochemistry. Hole-size selectivity for complexation of main group ions by polyoxo ionophores is well documented,⁶⁻⁸ although examples with transition metal ions are less common.^{6,12}

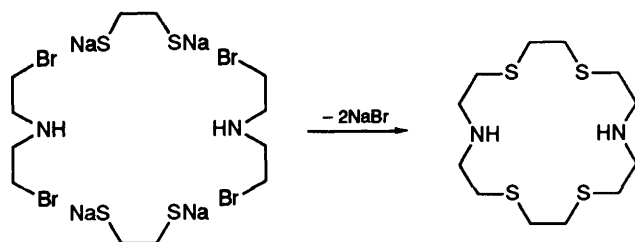
The aim of this review is to summarize the co-ordination chemistry of the mixed S- and N-donor macrocycles [18]aneN₂S₄ and Me₂[18]aneN₂S₄, the N₂S₄-donor analogues of 18-crown-6, [18]aneO₆. These ligands and their derivatives are attractive since they incorporate both hard (N) and soft (S-thioether) donor atoms. In principle, this may provide an effective system for monitoring the allosteric effects of binding hard main group and soft transition metal ions in close proximity.¹³ These mixed N/S donors may also generate complexes which model the active sites of certain redox-active metallo-proteins.¹⁴ Most importantly for us, however, the ligands [18]aneN₂S₄ and Me₂[18]aneN₂S₄ offer potential hexadentate co-ordination in a conformationally restricted environment. Binding of these ligands to an octahedral metal centre would generate complexes incorporating six, five-membered chelate rings. Encapsulation of a metal ion which is formally too large to fit with the hole size of these 18-membered ligands may constrict the metal ion, and/or twist and distort the ligand with an increase in ring strain.

We have been interested in the co-ordination chemistry of metal complexes in which the stereochemical preferences of the complexed metal ion are not compatible with the inherent conformational and configurational characteristics of the co-ordinating ligand(s).^{2,3} This stereochemical mis-match between metal(s) and ligand(s) is the basis of the 'entatic state' description of strained metal centres

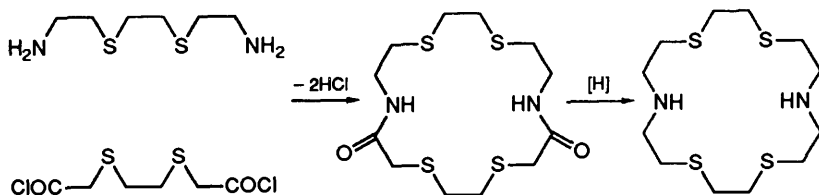
¹² D E Fenton, B P Murphey, A J Leong, L F Lindoy, A Bashall, and M McPartlin, *J Chem Soc Dalton Trans*, 1987, 2543, D E Fenton, *Pure Appl Chem*, 1986, **58**, 1437, L F Lindoy, *Prog Macrocycl Chem*, ed R Izatt and D Christensen, J Wiley, New York, 1987, 3 and references therein

¹³ D E Koshland, *Enzymes*, 3rd Edition, 1970, 1, 341, J Rebek, J E Trend, R V Whattley, and S Chakravor, *J Am Chem Soc*, 1979, **101**, 4333, J Rebek and L Marshall, *J Am Chem Soc*, 1983, **105**, 6668, J Rebek, *Acc Chem Res*, 1984, **17**, 258, N A Obaidi, P D Beer, J P Bright, C J Jones, J A McCleverty, and S S Salam, *J Chem Soc, Chem Commun*, 1986, 239, J-C Chambron and J-P Sauvage, *Tetrahedron Lett*, 1986, **27**, 865, A Hamilton, J-M Lehn, and J L Sessler, *J Am Chem Soc*, 1986, **108**, 5158, P D Beer, *J Chem Soc, Chem Commun*, 1986, 1678, C J van Staveren, D N Rheinhoudt, J van Eerden, and S Harkema, *J Chem Soc, Chem Commun*, 1987, 974, E Fu, M L H Green, V J Lowe, and S R Marder, *J Organomet Chem*, 1988, **341**, C39, P D Beer, H Sikanyika, A M S Slawin, and D J Williams, *Polyhedron*, 1989, **8**, 879 and references therein

¹⁴ N Atkinson, A J Blake, M G B Drew, G Forsyth, A J Lavery, G Reid, and M Schroder, *J Chem Soc, Chem Commun*, 1989, 984



Scheme 1 Synthesis of [18]aneN₂S₄¹⁶



Scheme 2 Synthesis of [18]aneN₂S₄¹⁷

at the active site of metallo-proteins such as azurin and plastocyanin.¹⁵ The distortion of metal co-ordination geometries can be monitored most readily by a combination of crystallographic and electrochemical studies, and this is the basis of the current study of the complexation chemistry of [18]aneN₂S₄ and Me₂[18]aneN₂S₄. While other mixed S- and N-donor macrocyclic complexes will be referred to, ligands comprising donor types other than sulphur and nitrogen will not be included.

2 Ligand Synthesis

The first synthesis of [18]aneN₂S₄ was reported by Black and co-workers in 1968.¹⁶ Reaction of 1,5-dibromo-3-azapentane with the disodium salt of ethane-1,2-dithiol in EtOH gave the free ligand as colourless needles in *ca.* 4.6% yield (Scheme 1). A templating agent was not utilized, and high-dilution techniques were therefore employed to encourage cyclization over linear polymerization. An alternative synthesis affording [18]aneN₂S₄ in 45% yield was reported later by Lehn and co-workers: this route employed high-dilution cyclization of the appropriate dithia-dicarboxylic acid dichloride with a dithia-diamine, followed by reduction of the resulting diamide (Scheme 2).¹⁷ This synthesis involves the use of mustard gas derivatives and therefore should be treated with utmost caution.

The single crystal *X*-ray structure of free [18]aneN₂S₄ shows the molecule

¹⁵ B. L. Vallee and R. J. P. Williams, *Biochemistry*, 1968, **59**, 498; R. J. P. Williams, *J. Mol. Cat., Review Issue*, 1986, 1.

¹⁶ D. St. C. Black and I. A. McLean, *J. Chem. Soc., Chem. Commun.*, 1968, 1004; *Tetrahedron Lett.*, 1969, 3961; *Aust. J. Chem.*, 1971, **24**, 1401.

¹⁷ B. Dietrich, J. M. Lehn, and J. P. Sauvage, *J. Chem. Soc., Chem. Commun.*, 1970, 1055.

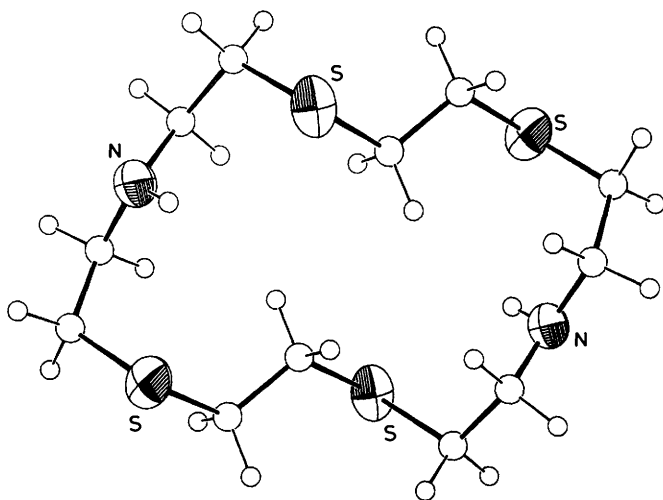


Figure 1 Crystal structure of [18]aneN₂S₄.¹⁸

lying across a crystallographic inversion centre, in a conformation resembling a figure-eight (Figure 1).¹⁸ Interestingly, the torsion angles at all four C–N bonds adopt *anti* placements, while all eight C–S linkages are *gauche*.¹⁸ Unlike the majority of metal-free thioether macrocycles such as [12]aneS₄,^{19, 20} [14]aneS₄,²¹ [15]aneS₅,²⁰ and [18]aneS₆,^{20, 22} which tend to adopt *exo*-configurations, the S-donor atoms in [18]aneN₂S₄ are neither *exo*- or *endo*-dentate. Instead the C–S–C triangle is almost perpendicular to the macrocyclic plane.

Me₂[18]aneN₂S₄ can be obtained in almost quantitative yield from [18]aneN₂S₄ by standard methylation procedures using formic acid and formaldehyde.²³ Lehn and co-workers have also reported the synthesis of a series of ‘face-to-face’ macrobicyclic and cryptand ligands involving mixed N- and S-donor macrocyclic subunits (Figure 2); these ligands can potentially act as binucleating agents.²⁴ An 18-membered ring, N₂S₄-donor macrocycle, L¹, incorporating a high degree of unsaturation has been reported by Lindoy and Busch.²⁵ Synthesis of this molecule is achieved by a template-mediated cyclization reaction of 1,2-

¹⁸ H L Ammon, K Chandrasekhar, S K Bhattacharjee, S Shinkai, and Y Honda, *Acta Crystallogr Sect C*, 1984, **40**, 2061

¹⁹ G H Robinson and S A Sangokoya, *J Am Chem Soc*, 1988, **110**, 1494

²⁰ R E Wolf, J R Hartman, J M E Storey, B M Foxman, and S R Cooper, *J Am Chem Soc*, 1987, **109**, 4328

²¹ L L Diaddario Jr, E R Dockal, M D Glick, L A Ochrymowycz, and D B Rorabacher, *Inorg Chem*, 1985, **24**, 356

²² J R Hartman, R E Wolf, B M Foxman, and S R Cooper, *J Am Chem Soc*, 1983, **105**, 131

²³ R N Icke, B B Wisegarver, and G A Alles, *Organic Synthesis Collected Volumes III*, 1955, 723

²⁴ A A Alberts, R Annunziata, and J M Lehn, *J Am Chem Soc*, 1977, **99**, 8502, O Kahn, I Morgenstern-Badarau, J P Audiere, and J M Lehn, *J Am Chem Soc*, 1980, **102**, 5936

²⁵ L F Lindoy and D H Busch, *J Chem Soc, Chem Commun*, 1968, 1598

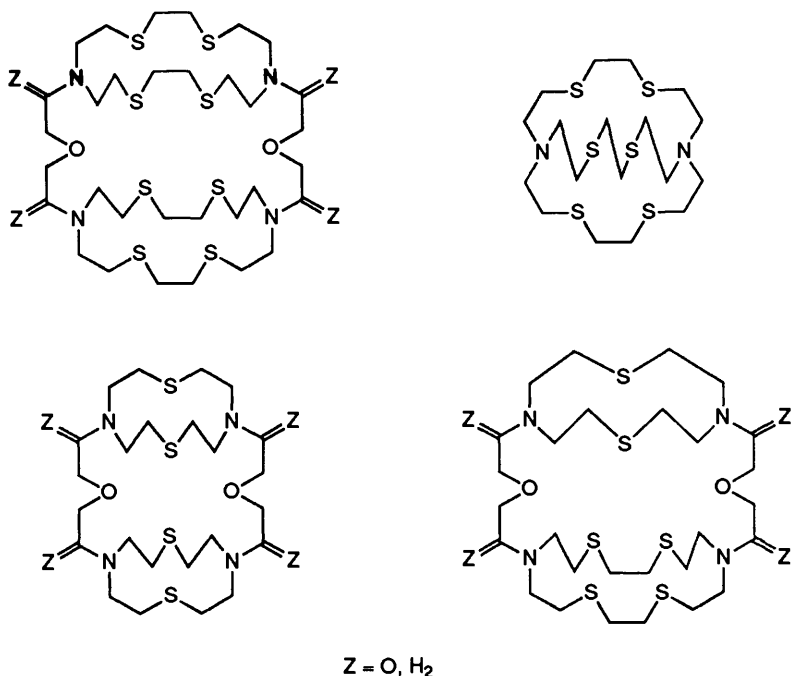
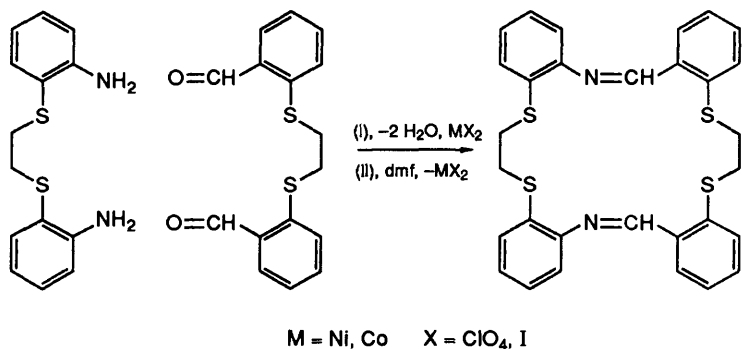


Figure 2 Face-to-face macrobicyclic ligands and cryptands^{17,24}



Scheme 3 Synthesis of L^{1,25}

bis(2-amino-phenylthio)ethane and 1,4-bis(2-formylphenyl)-1,4-dithiabutane (Scheme 3). It is proposed that due to the planarity of each S–N–S portion imposed by the conjugation, this macrocycle can only co-ordinate octahedrally in a *rac* configuration.

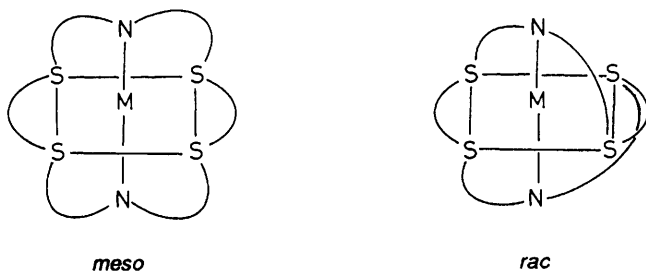


Figure 3 meso and rac Configurations for complexes $[M([18]aneN_2S_4)]^{x+}$

3 Co-ordination Complexes

In the first report of $[18]aneN_2S_4$ by Black and co-workers two possible conformations for a hexadentate ligand in an octahedral geometry were defined: mesomeric (*meso*) in which the two S–N–S linkages each bind facially to the metal centre, and racemic (*rac*) in which the two S–N–S portions each bind meridionally to the metal centre (Figure 3).¹⁶ A range of octahedral complexes $[M([18]aneS_6)]^{x+}$, $[M = Co^{II},^{26,27} Ni^{II},^{28,29} Cu^{II},^{30} Ru^{II},^{31} Pd^{II},^{32} Pt^{II},^{32} x = 2; M = Pd^{III},^{33} x = 3; M = Ag^I,^{34} x = 1]$ incorporating the hexathia analogue $[18]aneS_6$ have been structurally characterized. Without exception, the macrocycle in these complexes adopts a *meso* configuration thereby maximizing the number of *gauche* placements at the C–C–S–C linkages and thus avoiding unfavourable 1,4-interactions.^{4,20} This is not the case for co-ordination complexes of $[18]aneN_2S_4$.

A. Iron.—Reaction of $Fe(ClO_4)_2$ with one molar equivalent of $[18]aneN_2S_4$ in EtOH affords the low-spin, d^6 Fe^{II} complex $[Fe([18]aneN_2S_4)]^{2+}$ which can be isolated as a BPh_4^- or BF_4^- salt. The single crystal structure of this complex shows it to be the *rac* isomer with the Fe^{II} centre bound octahedrally *via* all six macrocyclic donor atoms, $Fe-S = 2.2578(17), 2.2588(16), 2.2673(16),$ and $2.2674(15) \text{ \AA}$, $Fe-N = 2.022(4)$ and $2.037(5) \text{ \AA}$ (Figure 4). The *rac* configuration observed for $[Fe([18]aneN_2S_4)]^{2+}$ reflects the preference for *gauche* torsions at C–S linkages and *anti* torsions at C–N (secondary amine) linkages. The single crystal X-ray structure of the hexathia analogue $[Fe([9]aneS_3)_2]^{2+}$ shows

²⁶ J R Hartman, E J Hints, and S R Cooper, *J Chem Soc, Chem Commun*, 1984, 386

²⁷ J R Hartman, E J Hints, and S R Cooper, *J Am Chem Soc*, 1986, **108**, 1208

²⁸ S R Cooper, S C Rawle, J R Hartman, E J Hints, and G A Admans, *Inorg Chem*, 1988, **27**, 1209

²⁹ S C Rawle, J R Hartman, D J Watkins, and S R Cooper, *J Chem Soc, Chem Commun*, 1986, 1083

³⁰ J R Hartman and S R Cooper, *J Am Chem Soc*, 1986, **108**, 1202

³¹ M N Bell, A J Blake, A J Holder, T I Hyde, and M Schroder, *J Chem Soc, Dalton Trans*, in press

³² A J Blake, R O Gould, A J Lavery, and M Schroder, *Angew Chem*, 1986, **98**, 282, *Angew Chem. Int Ed Engl*, 1986, **25**, 274

³³ A J Blake, A J Holder, T I Hyde, and M Schroder, unpublished results

³⁴ A J Blake, R O Gould, A J Holder, T I Hyde, and M Schroder, *Polyhedron*, 1989, **8**, 513

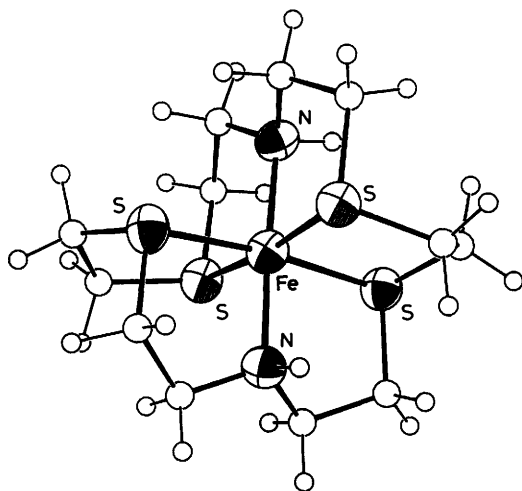


Figure 4 Crystal structure of $[\text{Fe}([\text{18]aneN}_2\text{S}_4)]^{2+}$

octahedral, low-spin Fe^{II} with facial binding of both $[\text{9]aneS}_3$ ligands, $\text{Fe-S} = 2.241(1)$, $2.251(1)$, and $2.259(1)\text{\AA}$.³⁵ The ligand $[\text{9]aneS}_3$ is pre-organized for facial co-ordination³⁶ and, therefore, the Fe-S bond lengths are likely to reflect a good fit of Fe^{II} with the two tridentate macrocycles. Noticeably, the Fe-S bond lengths are elongated in $[\text{Fe}([\text{18]aneN}_2\text{S}_4)]^{2+}$ and there is a small but significant tetrahedral distortion of the thioether S-donors out of the least-squares S_4 plane; this is a consequence of the small bite angle of the S-N-S portions and of the compression along the N-Fe-N axis. Thus, compression of the macrocycle along the N-Fe-N axis pushes the S-donors away from Fe^{II} and forces a small tetrahedral distortion in the S_4 plane. $[\text{Fe}([\text{18]aneN}_2\text{S}_4)]^{2+}$ shows an irreversible oxidation by cyclic voltammetry at $E_{\text{pa}} = +0.78\text{ V vs. Fc/Fc}^+$. This contrasts with $[\text{Fe}([\text{9]aneS}_3)_2]^{2+}$ which shows a reversible $\text{Fe}^{\text{II/III}}$ couple at $E_{\frac{1}{2}} = +0.98\text{ V vs. Fc/Fc}^+$.^{9,35}

B. Cobalt.—Treatment of $\text{Co}(\text{NO}_3)_2$ with one molar equivalent of $[\text{18]aneN}_2\text{S}_4$ in refluxing $\text{EtOH}/\text{H}_2\text{O}$ affords the purple complex $[\text{Co}([\text{18]aneN}_2\text{S}_4)]^{2+}$. The UV-vis spectrum of this complex is in accord with a low-spin, d^7 Co^{II} ion in an octahedral field,³⁵ which reflects the strong ligand-field imposed by the thioether S-donors. The electronic spectra and magnetic susceptibilities of the related species, $[\text{Co}([\text{9]aneS}_3)_2]^{2+}$ and $[\text{Co}([\text{9]aneN}_3)_2]^{2+}$ are consistent with low- and high-spin complexes respectively.^{35,37}

Aerial oxidation of an aqueous solution of $[\text{Co}([\text{18]aneN}_2\text{S}_4)]^{2+}$ yields a deep

³⁵ K. Wieghardt, H.-J. Küppers, and J. Weiss, *Inorg. Chem.*, 1985, **24**, 3067; H.-J. Küppers, A. Neves, C. Pomp, D. Ventur, K. Wieghardt, B. Nuber, and J. Weiss, *Inorg. Chem.*, 1986, **25**, 2400.

³⁶ R. S. Glass, G. S. Wilson, and W. N. Setzer, *J. Am. Chem. Soc.*, 1980, **102**, 5068.

³⁷ K. Wieghardt, W. Schmidt, W. Herrmann, and H. J. Küppers, *Inorg. Chem.*, 1983, **22**, 2953.

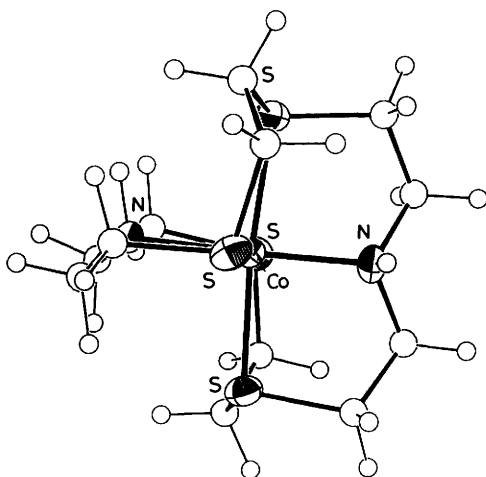


Figure 5 Crystal structure of $[\text{Co}([\text{18]aneN}_2\text{S}_4)]^{3+}$

Table 1 Redox couples for selected cobalt macrocyclic complexes

Complex	$E_{1/2}$ (V) ^a		Ref
	$\text{Co}^{\text{III/II}}$	$\text{Co}^{\text{II/I}}$	
$[\text{Co}([\text{18]aneN}_6)]^{2+}$	-0.868	—	27,39
$[\text{Co}([\text{9]aneN}_3)_2]^{2+}$	-1.13	—	27,35
$[\text{Co}([\text{18]aneN}_2\text{S}_4)]^{2+}$	-0.07	-1.30	this work
$[\text{Co}([\text{9]aneS}_3)_2]^{2+}$	-0.013	-0.86	35
$[\text{Co}([\text{18]aneS}_6)]^{2+}$	+0.124	-0.88 ^b	26,27
$[\text{Co}(\text{Me}_2[\text{18]aneN}_2\text{S}_4)]^{2+}$	+0.28	-0.99	this work

^a vs Fc/Fc^+ ^b Irreversible

red solution of $[\text{Co}([\text{18]aneN}_2\text{S}_4)]^{3+}$. The single crystal *X*-ray structure of this complex shows the d^6 Co^{III} ion co-ordinated to four S-donors and two mutually *trans* N-donors of the macrocycle in an octahedral stereochemistry, $\text{Co-S} = 2.2682(13), 2.2488(13), 2.2524(13), 2.2539(13)$, $\text{Co-N} = 1.993(4), 1.994(4)$ Å (Figure 5). The complex adopts the *rac* configuration, and there is a tetrahedral distortion of the S-donors out of the least-squares S_4 co-ordination plane. Interestingly, the low-spin, hexathia Co^{II} analogues show different structural features: octahedral $[\text{Co}([\text{18]aneS}_6)]^{2+}$ is tetragonally elongated, $\text{Co-S} = 2.251(1), 2.292(1), \text{and } 2.479(1)$ Å with the complex adopting a *meso* configuration,^{26,27} while the single crystal *X*-ray structure of $[\text{Co}([\text{9]aneS}_3)_2]^{2+}$ shows a tetragonally compressed octahedral stereochemistry, $\text{Co-S} = 2.240(7), 2.356(6), \text{and } 2.367(5)$ Å.³⁸

Table 1 summarizes voltammetric data for a series of cobalt macrocyclic com-

³⁸ W N Setzer, C A Ogle, G S Wilson, and R S Glass, *Inorg Chem*, 1983, **22**, 266

³⁹ R W Hay, B Jeragh, S F Lincoln, and G H Searle, *Inorg Nucl Chem Letts*, 1978, **14**, 435

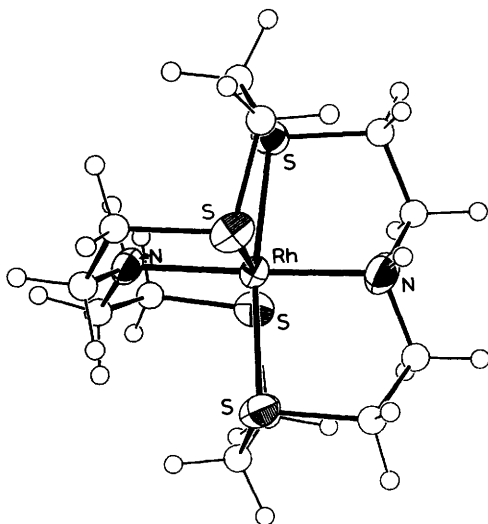


Figure 6 Crystal structure of $[\text{Rh}([\text{18}]\text{aneN}_2\text{S}_4)]^{3+}$

plexes. Cyclic voltammetry of $[\text{Co}([\text{18}]\text{aneN}_2\text{S}_4)]^{2+}$ shows two reversible, one-electron redox processes at $E_{\frac{1}{2}} = -0.07 \text{ V}$ and $-1.30 \text{ V vs Fc/Fc}^+$ assigned to $\text{Co}^{\text{II/III}}$ and $\text{Co}^{\text{III/I}}$ couples respectively. The potential for the $[\text{Co}([\text{18}]\text{aneN}_2\text{S}_4)]^{2+/3+}$ redox couple is slightly less anodic than that for $[\text{Co}([\text{18}]\text{aneS}_6)]^{2+/3+}$, while the reduction is considerably more cathodic. Interestingly, the $\text{Co}^{\text{II/III}}$ couples for $[\text{Co}([\text{18}]\text{aneN}_2\text{S}_4)]^{2+}$ and $[\text{Co}([\text{9}]\text{aneS}_3)_2]^{2+}$ are very similar. An N_2S_4 - or N_6 -donor ligand would be expected to stabilize Co^{III} and destabilize Co^{I} compared to an S_6 -donor set. This is the case for the complexes in Table 1; however, it appears that this effect is counter-balanced for $[\text{Co}([\text{18}]\text{aneN}_2\text{S}_4)]^{2+}$ and $[\text{Co}([\text{9}]\text{aneS}_3)_2]^{2+}$ by the relative conformational rigidity of $[\text{18}]\text{aneN}_2\text{S}_4$. The $\text{Co}^{\text{II/III}}$ and $\text{Co}^{\text{III/I}}$ couples for $[\text{Co}(\text{Me}_2[\text{18}]\text{aneN}_2\text{S}_4)]^{2+}$, $E_{\frac{1}{2}} = +0.28 \text{ V}$ and $-0.99 \text{ V vs Fc/Fc}^+$ respectively, occur at much more anodic potentials compared to those for $[\text{Co}([\text{18}]\text{aneN}_2\text{S}_4)]^{2+}$, suggesting greater interaction of the soft thioether donors with the metal centre in the former complex.

C. Rhodium.—Treatment of RhCl_3 with *ca.* 3.2 equivalents of TIPF_6 and one molar equivalent of $[\text{18}]\text{aneN}_2\text{S}_4$ in refluxing CH_3CN affords $[\text{Rh}([\text{18}]\text{aneN}_2\text{S}_4)](\text{PF}_6)_3$ as an orange solid. Synthesis of this compound can also be achieved by reaction of $[\text{Rh}(\text{H}_2\text{O})_6]^{3+}$ with $[\text{18}]\text{aneN}_2\text{S}_4$ in refluxing $\text{MeOH}/\text{H}_2\text{O}$. The PF_6^- salt shows particularly low solubility in organic solvents. The single crystal *X*-ray structure of this complex (Figure 6) shows the d^6 Rh^{III} ion co-ordinated to all six macrocyclic donor atoms in a *rac* configuration, giving an overall geometry very similar to that determined for $[\text{Co}([\text{18}]\text{aneN}_2\text{S}_4)]^{3+}$ and $[\text{Fe}([\text{18}]\text{aneN}_2\text{S}_4)]^{2+}$. The Rh-S and Rh-N bond lengths, $\text{Rh-S} =$

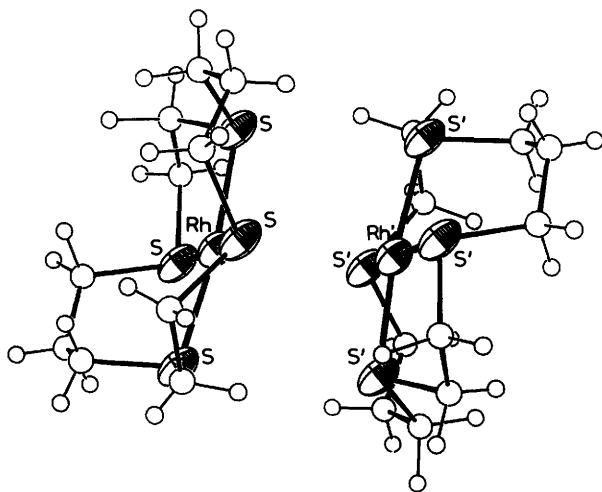


Figure 7 Crystal structure of $[\text{Rh}([\text{14]aneS}_4)]^+$

2.3289(14), 2.3349(14), 2.3353(14), and 2.3416(14) Å, Rh–N = 2.083(4) and 2.101(5) Å are similar to those observed in related complexes such as $[\text{Rh}([\text{9]aneS}_3)_2]^{3+}$, Rh–S = 2.3316(14), 2.3335(12), and 2.3335(12) Å^{40,41} and $[\text{Rh}([\text{9]aneN}_3)_2]^{3+}$, Rh–N = 2.058(18), 2.065(19), and 2.073(21) Å.^{42,43} $[\text{Rh}([\text{18]aneN}_2\text{S}_4)]^{3+}$ represents the first characterized complex of Rh^{III} encapsulated octahedrally by co-ordination to an 18-membered ring macrocycle.

Cyclic voltammetry of $[\text{Rh}([\text{18]aneN}_2\text{S}_4)](\text{BPh}_4)_3$ shows a broad, irreversible reduction at $E_{pc} = -1.34 \text{ V vs Fc/Fc}^+$ tentatively assigned to the formation of a d^8 Rh^I species. A Rh^I tetrathia macrocyclic complex, $[\text{Rh}([\text{14]aneS}_4)]^+$ has been reported previously, and shows square planar co-ordination to Rh^I via four S-donors, Rh–S = 2.261(3)–2.285(4) Å, with the metal ion displaced from the S₄ co-ordination plane by 0.133(2) Å towards a second $[\text{Rh}([\text{14]aneS}_4)]^+$ cation, Rh...Rh = 3.313(1), Rh...S = 3.697(9)–3.822(3) Å (Figure 7).⁴⁴

The complex $[\text{Rh}([\text{9]aneS}_3)_2]^{3+}$ exhibits very different redox characteristics to $[\text{Rh}([\text{18]aneN}_2\text{S}_4)]^{3+}$. $[\text{Rh}([\text{9]aneS}_3)_2]^{3+}$ shows a reversible Rh^{III/II} couple at $E_{1/2} = -0.71 \text{ V vs Fc/Fc}^+$. The reduction product has been confirmed as the mononuclear d^7 Rh^{II} cation, $[\text{Rh}([\text{9]aneS}_3)_2]^{2+}$, by ESR and *in situ* UV-vis spectroscopy.⁴¹ A reversible Rh^{III/I} couple is also evident for this system at $E_{1/2} = -1.08 \text{ V vs Fc/Fc}^+$. Interestingly, the stabilization of low-valent Rh centres is not

⁴⁰ A J Blake, A J Holder, T I Hyde, and M Schroder, *J Chem Soc., Chem Commun.*, 1987, 987

⁴¹ S C Rawle, R Yagbasan, K Prout, and S R Cooper, *J Am Chem Soc.*, 1987, **109**, 6181, A J Blake R O Gould, A J Holder, T I Hyde, and M Schroder, *J Chem Soc., Dalton Trans.*, 1988, 1861

⁴² A J Blake, T I Hyde, and M Schroder, unpublished results

⁴³ K Wiegardt, W Schmidt, B Nuber, B Prikner, and J Weiss, *Chem Ber.*, 1980, **113**, 36

⁴⁴ T Yoshida, T Ueda, T Adachi, K Yamamoto, and T Higuchi, *J Chem Soc., Chem Commun.*, 1985, 1137

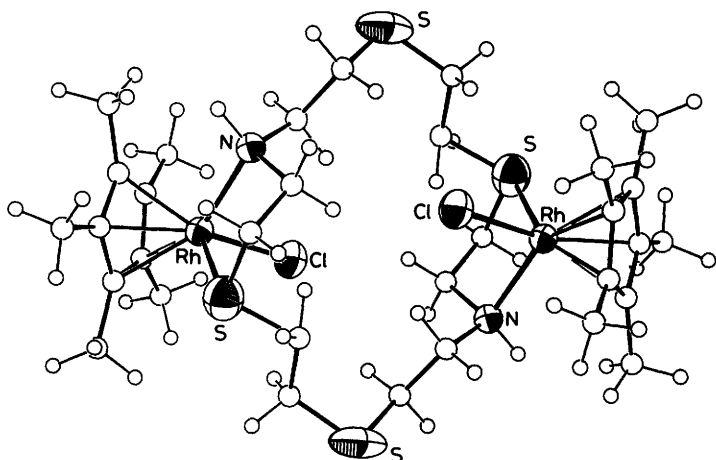


Figure 8 Crystal structure of $[\text{Rh}_2([\text{18}]\text{aneN}_2\text{S}_4)\text{Cl}_2(\text{C}_5\text{Me}_5)_2]^{2+}$

achieved by the analogous bis(triaza) complex, $[\text{Rh}([\text{9}]\text{aneN}_3)_2]^{3+}$; this complex shows two irreversible reductions at much more cathodic potentials, $E_{\text{pc}} = -1.93$ and -2.32 V vs Fc/Fc^+ .⁴²

The synthesis of an unusual binuclear Rh^{III} complex incorporating $[\text{18}]\text{aneN}_2\text{S}_4$ has also been achieved. Treatment of $[\text{RhCl}_2(\text{C}_5\text{Me}_5)_2]$ with one molar equivalent of $[\text{18}]\text{aneN}_2\text{S}_4$ in refluxing CH_3OH affords⁴⁵ the complexation $[\text{Rh}_2\text{Cl}_2(\text{C}_5\text{Me}_5)_2([\text{18}]\text{aneN}_2\text{S}_4)]^{2+}$. The single crystal X-ray structure of this complex shows each chiral Rh^{III} centre bound to one S- and one N-donor of the macrocycle, $\text{Rh}-\text{S} = 2.3739(23)$, $\text{Rh}-\text{N} = 2.296(4)$ Å, one Cl^- ligand, $\text{Rh}-\text{Cl} = 2.3829(18)$ Å, and bound facially to a C_5Me_5^- ligand (Figure 8). Therefore, $[\text{18}]\text{aneN}_2\text{S}_4$ acts as a bidentate ligand, bridging two Rh^{III} centres, and leaving two thioether S-donors unco-ordinated.⁴⁵ A similar structure has been observed for $[\text{Rh}_2\text{Cl}_2(\text{C}_5\text{Me}_5)_2([\text{18}]\text{aneS}_6)]^{2+}$ which shows octahedral coordination about Rh^{III} via two S-donors of $[\text{18}]\text{aneS}_6$, $\text{Rh}-\text{S} = 2.2364(10)$ and $2.3764(10)$ Å, one Cl^- ligand, $\text{Rh}-\text{Cl} = 2.3865(10)$ Å, and a facially co-ordinated C_5Me_5^- ligand.^{3,46} Analogous complexes with $[\text{14}]\text{aneS}_4$ and $[\text{18}]\text{aneN}_6$ have been prepared.^{3,45}

A stable binuclear Rh^{I} complex incorporating another N_2S_4 -donor macrocycle, $[\text{Rh}_2(\text{CO})_2(\text{L}^2)]^{2+}$ has been reported.⁴⁷ In this case co-ordination to each Rh^{I} centre is proposed to be via a square planar arrangement of two macrocyclic S-donors, one macrocyclic N-donor and one CO ligand, with the S-N-S linkage of L^2 bound meridionally to each Rh^{I} centre (Figure 9). The synthesis and structure

⁴⁵ M. N. Bell, PhD Thesis, University of Edinburgh, 1987.

⁴⁶ M. N. Bell, A. J. Blake, M. Schröder, and T. A. Stephenson, *J. Chem. Soc., Chem. Commun.*, 1986, 471.

⁴⁷ D. Parker, J. M. Lehn, and J. Rimmer, *J. Chem. Soc., Dalton Trans.*, 1985, 1517. See also: G. Ferguson, K. E. Matthes, and D. Parker, *J. Chem. Soc., Chem. Commun.*, 1987, 1350.

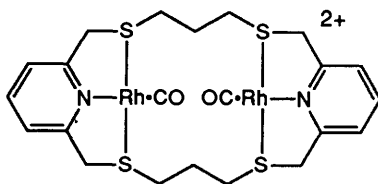


Figure 9 Diagram of $[\text{Rh}_2\text{CO}_2(\text{L}^2)]^{2+}$

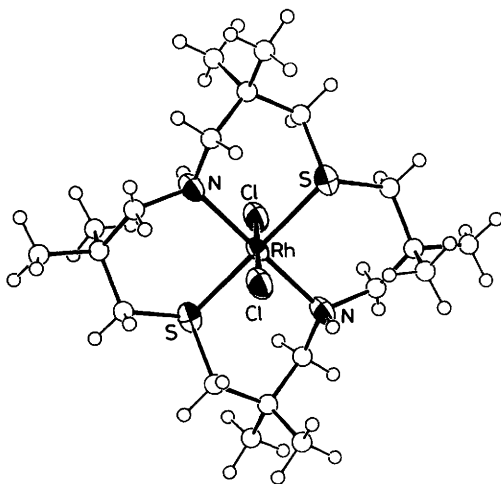


Figure 10 Crystal structure of $[\text{RhCl}_2(\text{L}^3)]^+$

of a Rh^{III} complex incorporating the N_2S_2 -donor macrocycle, L^3 , has also been described.⁴⁸ Preparation of $[\text{RhCl}_2(\text{L}^3)]^+$ is achieved by reaction of RhCl_3 with L^3 in refluxing EtOH. The single crystal structure of this species shows two independent cations, each of which adopts a distorted octahedral geometry at Rh^{III} through equatorial co-ordination to the four macrocyclic donor atoms, $\text{Rh-S} = 2.303(4)$ and $2.344(3)$ Å; $\text{Rh-N} = 2.260(5)$ and $2.132(8)$ Å, and apical co-ordination to two mutually trans Cl^- ligands, $\text{Rh-Cl} = 2.308(3)$ and $2.325(3)$ Å (Figure 10).⁴⁸ In both forms of the cation the macrocyclic ring adopts a chair, twist-boat conformation, the only difference being the degree of twist in two of the chelate rings. A similar *trans*-dichloro structure has been observed for $[\text{RhCl}_2([\text{16}] \text{aneS}_4)]^+$; in contrast, $[\text{RhCl}_2([\text{14}] \text{aneS}_4)]^+$ and $[\text{RhCl}_2([\text{12}] \text{aneS}_4)]^+$ both exist exclusively as the *cis*-dichloro isomers, due to the smaller macrocyclic cavity size.⁴⁹

D. Nickel.—Treatment of $\text{Ni}(\text{NO}_3)_2$ with one molar equivalent of $[\text{18}] \text{aneN}_2\text{S}_4$

⁴⁸ R McCrindle, G Ferguson, A J McAlees, M Parvez, B L Ruhl, D K Stephenson, and T Wieckowski, *J Chem Soc, Dalton Trans*, 1986, 2351

⁴⁹ A J Blake, G Reid, and M Schroder, *J Chem Soc, Dalton Trans*, 1989, 1675

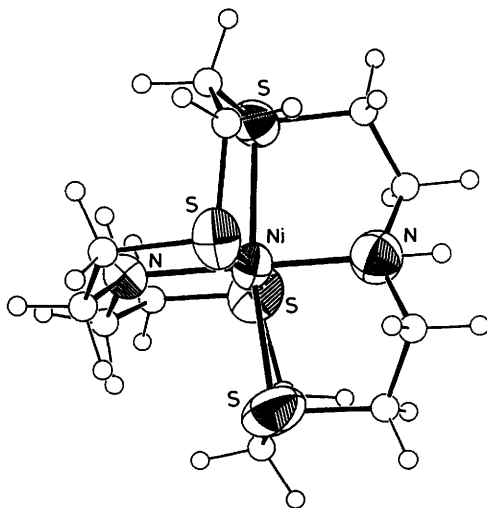


Figure 11 Crystal structure of $[\text{Ni}([\text{18}]\text{aneN}_2\text{S}_4)]^{2+}$

in refluxing $\text{H}_2\text{O}/\text{EtOH}$ affords $[\text{Ni}([\text{18}]\text{aneN}_2\text{S}_4)]^{2+}$, the structure of which shows Ni^{II} binding to an octahedral arrangement of all six donors of the macrocycle in a *rac* configuration, $\text{Ni}-\text{S} = 2.403(6)$, $2.407(5)$, $2.416(7)$, and $2.430(5)$; $\text{Ni}-\text{N} = 2.065(13)$ and $2.126(13)$ Å (Figure 11). These bond lengths are very similar to those observed for $[\text{Ni}([\text{9}]\text{aneN}_2\text{S}_2)]^{2+}$: $\text{Ni}-\text{S} = 2.418(1)$, $\text{Ni}-\text{N} = 2.108(2)$, $2.122(2)$ Å.⁵⁰ By contrast, $[\text{Ni}([\text{18}]\text{aneS}_6)]^{2+}$ adopts a *meso* conformation with shorter $\text{Ni}-\text{S}$ bond lengths, $\text{Ni}-\text{S} = 2.377(1)$, $2.389(1)$, and $2.397(1)$ Å.^{28,29} A similar compression in $\text{Ni}-\text{S}$ bond lengths is observed in the bis-sandwich complex, $[\text{Ni}([\text{9}]\text{aneS}_3)_2]^{2+}$, where each ligand binds facially to Ni^{II} , $\text{Ni}-\text{S} = 2.377(1)$, $2.380(1)$, and $2.400(1)$ Å.³⁸ Interestingly, the crystal structure of $[\text{Ni}([\text{12}]\text{aneS}_3)_2]^{2+}$ shows significantly longer $\text{Ni}-\text{S}$ bond lengths than $[\text{Ni}([\text{9}]\text{aneS}_3)_2]^{2+}$, $\text{Ni}-\text{S} = 2.409(1)$, $2.421(2)$, and $2.435(1)$ Å,^{28,51} and the larger ring macrocycle, $[\text{24}]\text{aneS}_6$, co-ordinates octahedrally to Ni^{II} to give a *rac* isomer with uncompressed $\text{Ni}-\text{S}$ bond lengths, $\text{Ni}-\text{S} = 2.413(1)$, $2.437(1)$, and $2.443(1)$ Å.^{28,29} These effects are related to the greater ring sizes in these crown complexes. Consistent with the other octahedral complexes of $[\text{18}]\text{aneN}_2\text{S}_4$, $[\text{Ni}([\text{18}]\text{aneN}_2\text{S}_4)]^{2+}$ exhibits a tetrahedral distortion of the S-atoms out of the least-squares S_4 co-ordination plane.

$[\text{Ni}([\text{18}]\text{aneN}_2\text{S}_4)]^{2+}$ shows two reversible one-electron redox processes at $E_{\frac{1}{2}} = +0.98$ and -1.51 V vs Fc/Fc^+ assigned to $\text{Ni}^{\text{II/III}}$ and $\text{Ni}^{\text{II/I}}$ couples respectively. The ESR spectrum of the Ni^{III} species $[\text{Ni}([\text{18}]\text{aneN}_2\text{S}_4)]^{3+}$, prepared by controlled potential oxidation of $[\text{Ni}([\text{18}]\text{aneN}_2\text{S}_4)]^{2+}$, shows a

⁵⁰ S. M. Hart, J. C. A. Boeyens, J. P. Michael, and R. D. Hancock, *J. Chem. Soc., Dalton Trans.*, 1983, 1601.

⁵¹ W. Rosen and D. H. Busch, *Inorg. Chem.*, 1970, 9, 262.

Table 2 Electronic spectral and redox data for octahedral nickel macrocyclic complexes

Complex	10Dq (cm ⁻¹)	$E_{\frac{1}{2}}$ Ni ^{II/III} (V) ^a	Ref
[Ni([9]aneS ₃) ₂] ²⁺	12 755	+0.97	35
[Ni([9]aneN ₃) ₂] ²⁺	12 500	+0.558	56,57,58
[Ni([18]aneS ₆) ₂] ²⁺	12 290		29
[Ni([18]aneN ₂ S ₄) ₂] ²⁺	12 135	+0.98	this work
[Ni([9]aneN ₂ S) ₂] ²⁺	11 770	+0.785	57,58
[Ni([9]aneN ₂ O) ₂] ²⁺	11 600	+1.084	57,58
[Ni([12]aneS ₃) ₂] ²⁺	11 240		28
[Ni([18]aneN ₆) ₂] ²⁺	11 200	+0.80	28,53,59
[Ni(Me ₂ [18]aneN ₂ S ₄) ₂] ²⁺	11 075	+1.51(t) ^b	this work
[Ni([24]aneS ₆) ₂] ²⁺	11 050		29

^a vs Fc/Fc⁺ ^b (t) Irreversible

strong rhombic signal at $g_1 = 2.129$, $g_2 = 2.104$, and $g_3 = 2.027$. [Ni([9]aneS₃)₂]²⁺ shows a reversible Ni^{II/III} and a quasi-reversible Ni^{II/I} couple at $E_{\frac{1}{2}} = +0.97\text{V}$ and -1.11V vs Fc/Fc⁺ respectively.^{55,52} These results parallel the Co systems in the sense that both Co^I and Ni^I are better stabilized by S₆ than by N₂S₄ macrocycles. However, the differences between the M^{II/III} couples for [M([9]aneS₃)₂]²⁺ and [M([18]aneN₂S₄)₂]²⁺ (M = Co, Ni) are much smaller; indeed for Ni, it appears that unstrained S₆ co-ordination in [Ni([9]aneS₃)₂]²⁺ stabilizes Ni^{III} as effectively as the conformationally restricted N₂S₄-ligand in [Ni([18]aneN₂S₄)₂]²⁺. Interestingly, an anodic shift in the Ni^{II/III} couple is noted⁵³ on going from [Ni([9]aneN₃)₂]²⁺ to the conformationally restricted [Ni([18]aneN₆)₂]²⁺. Trivalent nickel species are of interest as models for nickel-containing hydrogenase enzymes.⁵⁴ Recent studies on model systems have led to the re-interpretation of ESR spectral data, previously assigned to Ni^{III} radicals, as ligand-thiolate radicals.⁵⁵ Our own data might therefore be interpreted as indicating the formation of S-based radical cations, but additional results on [Ni(Me₂[18]aneN₂S₄)₂]²⁺ suggest that these redox potentials refer to genuine metal-based processes.

Reaction of Ni(NO₃)₂ with one molar equivalent of Me₂[18]aneN₂S₄ in refluxing EtOH/H₂O affords [Ni(Me₂[18]aneN₂S₄)₂]²⁺. UV-vis spectroscopy

⁵² A J Holder, PhD Thesis, University of Edinburgh, 1987

⁵³ A Bencini, L Fabbrizzi, and A Poggi, *Inorg Chem*, 1981, **20**, 2544, A Buttafava, L Fabbrizzi, A Perotti, A Poggi, G Poli, and B Seghi, *Inorg Chem*, 1986, **25**, 1456

⁵⁴ A J Thomson, *Nature (London)*, 1982, **298** 602, Y Sigiura, J Kuwahara, and T Suzuki, *Biochem Biophys Res Commun*, 1983, **115**, 878, S P J Albracht, J W van der Zwaan, and R D Fontijn, *Biochim Biophys Acta*, 1984, **766**, 245, S P J Albracht, R D Fontijn, and J W van der Zwaan, *Biochim Biophys Acta*, 1985, **832**, 89, J W van der Zwaan, S P J Albracht, R D Fontijn, and E C Slater, *FEBS Lett*, 1985, **179**, 271, J W van der Zwaan, S P J Albracht, R D Fontijn, and Y B M Roelofs, *Biochim Biophys Acta*, 1986, **872**, 208, R H Crabtree, *Inorg Chim Acta*, 1986, **125**, L7

⁵⁵ M Kumar, R O Day, G J Colpas, and M J Maroney, *J Am Chem Soc*, 1989, **111**, 5974, M Kumar, G J Colpas, R O Day, and M J Maroney, *J Am Chem Soc*, 1989, **111**, 8323

⁵⁶ R Yang and L Zompa, *Inorg Chem*, 1976, **15**, 1499

⁵⁷ L Fabbrizzi and D M Proserpio, *J Chem Soc, Dalton Trans*, 1989, 229

⁵⁸ S M Hart, J C A Boeyens, and R D Hancock, *Inorg Chem*, 1983, **22**, 982

⁵⁹ A Bencini, L Fabbrizzi, and A Poggi, *Inorg Chem*, 1981, **20**, 2544

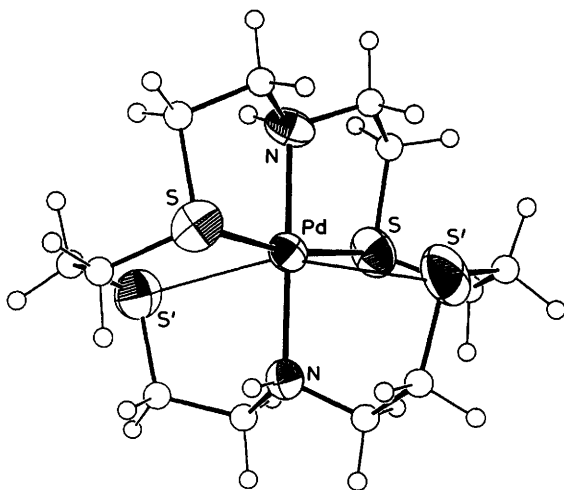


Figure 12 Crystal structure of $[\text{Pd}([\text{18]aneN}_2\text{S}_4)]^{2+}$

gives a value for $10Dq$ of $11\,075\text{ cm}^{-1}$ for this complex which is lower than for the non-methylated analogue, $[\text{Ni}([\text{18]aneN}_2\text{S}_4)]^{2+}$ (Table 2). The data summarized in Table 2 suggest that conformational and stereochemical considerations as well as S- or N-donacity are important in terms of quantifying $10Dq$ and the redox potentials. The cyclic voltammogram of $[\text{Ni}(\text{Me}_2[\text{18]aneN}_2\text{S}_4)]^{2+}$ exhibits a reversible, one-electron reduction at $E_{\frac{1}{2}} = -1.16\text{ V vs Fc/Fc}^+$ assigned to a $\text{Ni}^{\text{II/I}}$ couple. This reduction potential is considerably more anodic than for $[\text{Ni}([\text{18]aneN}_2\text{S}_4)]^{2+}$, strongly suggesting a greater interaction of the central metal ion with the soft thioether S-donors, and less interaction with the N-donors in $[\text{Ni}(\text{Me}_2[\text{18]aneN}_2\text{S}_4)]^{2+}$ compared to $[\text{Ni}([\text{18]aneN}_2\text{S}_4)]^{2+}$. Consistent with this, $[\text{Ni}(\text{Me}_2[\text{18]aneN}_2\text{S}_4)]^{2+}$ shows a highly anodic oxidation at $E_{\text{pa}} = +1.51\text{ V}$ by cyclic voltammetry. In addition, an irreversible reduction is observed at $E_{\text{pc}} = -2.17\text{ V vs Fc/Fc}^+$ tentatively assigned to a $\text{Ni}^{\text{II/0}}$ couple. On the basis of these data, and by comparison with the Cu^{II} and Ag^{I} complexes of $\text{Me}_2[\text{18]aneN}_2\text{S}_4$ (see below), we assign $[\text{Ni}(\text{Me}_2[\text{18]aneN}_2\text{S}_4)]^{2+}$ as a *meso* complex.

E. Palladium.—Reaction of PdCl_2 with one molar equivalent of $[\text{18]aneN}_2\text{S}_4$ in refluxing CH_3CN in the presence of *ca.* 2.2 molar equivalents of TIPF_6 affords the purple species $[\text{Pd}([\text{18]aneN}_2\text{S}_4)]^{2+}$. The single crystal *X*-ray structure of $[\text{Pd}([\text{18]aneN}_2\text{S}_4)]^{2+}$ shows a highly unusual distorted octahedral stereochemistry (Figure 12). Co-ordination to the d^8 Pd^{II} ion is *via* a square planar N_2S_2 donor set, $\text{Pd-S} = 2.311(3)$ and $2.357(3)\text{ \AA}$; $\text{Pd-N} = 2.068(7)$ and $2.123(7)\text{ \AA}$.⁶⁰ In addition, the two remaining thioether S-donors interact at long-

⁶⁰ G. Reid, A. J. Blake, T. I. Hyde, and M. Schröder, *J. Chem. Soc., Chem. Commun.*, 1988, 1397; A. J. Blake, G. Reid, and M. Schröder, *J. Chem. Soc., Dalton Trans.*, in press.

range with the metal centre, Pd \cdots S = 2.954(4) and 3.000(3) Å, and are displaced from the least-squares [PdN₂S₂]²⁺ co-ordination plane in opposite directions by 2.863 and 2.901 Å. A similar weak, long-range interaction has been observed previously⁶¹ in [Pd([9]aneS₃)₂]²⁺. This cation exhibits four normal Pd–S_{equ} bond lengths, Pd–S_{equ} = 2.332(3) and 2.311(3) Å, and two much weaker interactions of the apical thioethers, Pd \cdots S_{ap} = 2.952(4) Å. The complex [Pd([18]aneS₆)](BPh₄)₂ adopts a different stereochemistry, with the macrocycle forming an S-shaped double-boat conformation involving equatorial Pd–S bonds of 2.3114(14), 2.3067(15) Å, and long-range weak interaction of the two apical S-donors, Pd \cdots S_{ap} = 3.2730(17) Å.³²

Cyclic voltammetry of [Pd([18]aneN₂S₄)]²⁺ shows a chemically reversible one-electron oxidation at $E_{\frac{1}{2}} = +0.57$ V vs Fc/Fc⁺. Electrochemical oxidation of [Pd([18]aneN₂S₄)]²⁺ yields a bright red solution of [Pd([18]aneN₂S₄)]³⁺. ESR spectroscopy confirms this as a predominantly metal-based oxidation, showing a strong rhombic signal with $g_1 = 2.064$, $g_2 = 2.052$, and $g_3 = 2.019$. *In situ* UV-vis spectroscopy shows that oxidation of [Pd([18]aneN₂S₄)]²⁺ occurs reversibly and isospectically.⁶⁰ Reversible Pd^{II/III} couples have been reported for the related complexes, [Pd([9]aneS₃)₂]²⁺, ($E_{\frac{1}{2}} = +0.605$ V vs Fc/Fc⁺)⁴⁰ and [Pd([9]aneN₃)₂]²⁺, ($E_{\frac{1}{2}} = +0.07$ V vs Fc/Fc⁺).^{62,63} The oxidation products, [Pd([9]aneS₃)₂]³⁺⁴⁰ and [Pd([9]aneN₃)₂]³⁺⁶² have both been structurally characterized by single crystal X-ray diffraction. Both structures show tetragonally elongated octahedral stereochemistries at Pd^{III}, Pd–S_{equ} = 2.332(3) and 2.311(3) Å; Pd \cdots S_{ap} = 2.952(4) Å for [Pd([9]aneS₃)₂]³⁺, Pd–N = 2.111(9), 2.118(9), and 2.180(9) Å for [Pd([9]aneN₃)₂]³⁺. The stabilization of Pd^{III} by these macrocyclic ligands and also by [18]aneN₂S₄ is attributed to the availability of six-donor atoms in a conformation allowing a distorted octahedral stereochemistry at the d⁷ Pd^{III} ion.⁶⁰

Synthesis of the di-*N*-methylated analogue of [Pd([18]aneN₂S₄)]²⁺, [Pd(Me₂[18]aneN₂S₄)]²⁺, is achieved by reaction of PdCl₂ with one molar equivalent of Me₂[18]aneN₂S₄ in refluxing CH₃CN/H₂O. A single crystal X-ray structure of [Pd(Me₂[18]aneN₂S₄)]²⁺ shows the complex to have a completely different stereochemistry to [Pd([18]aneN₂S₄)]²⁺; [Pd(Me₂[18]aneN₂S₄)]²⁺ incorporates square planar co-ordination of the four thioether S-donors of the macrocycle to the Pd^{II} ion, Pd–S = 2.3239(22), 2.3261(22), 2.3331(22), and 2.3399(22) Å (Figure 13).⁶⁰ Notably, the two N–Me functions are directed away from the metal centre and do not interact, Pd \cdots N = 3.744(7) and 3.760(6) Å. The ligand Me₂[18]aneN₂S₄, therefore, co-ordinates to Pd^{II} as a simple tetradentate thioether-donor.

⁶¹ K Wiegardt, H-J Kuppers, E Raabe, and C Kruger, *Angew Chem*, 1986, **98**, 1136. *Angew Chem. Int Ed Engl*, 1986, **25**, 1101. A J Blake, A J Holder, T I Hyde, Y V Roberts, A J Lavery, and M Schroder *J Organomet Chem*, 1987, **323**, 261

⁶² A J Blake, L M Gordon, A J Holder, T I Hyde, G Reid, and M Schroder. *J Chem Soc., Chem Commun*, 1988, 1452

⁶³ A McAuley, T W Whitcombe, and G Hunter, *Inorg Chem*, 1988, **27**, 2634. A McAuley and T W Whitcombe, *Inorg Chem*, 1988, **27**, 3090

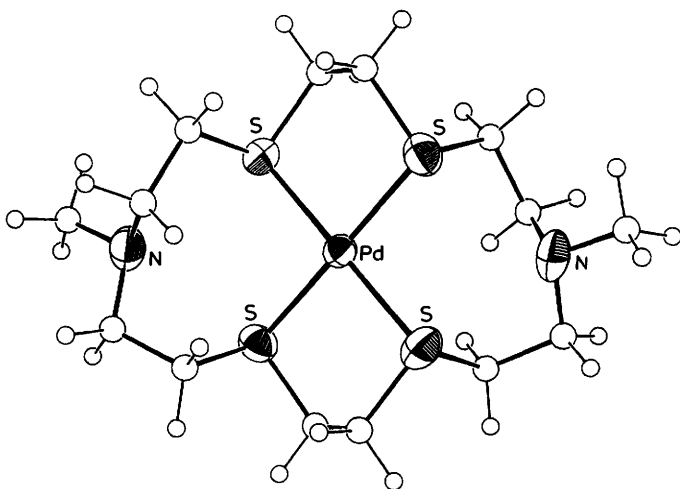


Figure 13 Crystal structure of $[\text{Pd}(\text{Me}_2[18]\text{aneN}_2\text{S}_4)]^{2+}$

Comparison of the structures of $[\text{Pd}([18]\text{aneN}_2\text{S}_4)]^{2+}$ and $[\text{Pd}(\text{Me}_2[18]\text{aneN}_2\text{S}_4)]^{2+}$ demonstrates that replacement of N–H by N–Me moieties has a remarkable influence on the stereochemistry adopted by the complex. This difference is associated mainly with the steric bulk of the N–Me groups, and is reflected in the redox characteristics of the parent Pd^{II} complexes.

Cyclic voltammetry of $[\text{Pd}(\text{Me}_2[18]\text{aneN}_2\text{S}_4)]^{2+}$ shows a chemically reversible one-electron reduction at $E_{\frac{1}{2}} = -0.74 \text{ V vs Fc/Fc}^+$ assigned to a $\text{Pd}^{\text{II/I}}$ couple. Electrochemical reduction of this species yields the bright yellow d^9 Pd^{I} complex, $[\text{Pd}(\text{Me}_2[18]\text{aneN}_2\text{S}_4)]^+$. Reduction to $[\text{Pd}(\text{Me}_2[18]\text{aneN}_2\text{S}_4)]^+$ occurs reversibly and isobestically, as shown by *in situ* UV-vis spectroscopy.⁶⁰ Assignment of this product as a genuine monomeric Pd^{I} species is possible on the basis of ESR spectroscopy. The ESR spectrum of $[\text{Pd}(\text{Me}_2[18]\text{aneN}_2\text{S}_4)]^+$ shows a strong anisotropic signal giving $g_{\parallel} = 2.155$, $g_{\perp} = 2.049$, with hyperfine coupling to ^{105}Pd ($I = 5/2$, 22.2%), $A_{\parallel} = 48\text{G}$, $A_{\perp} = 34\text{G}$. Similar spectral characteristics have been observed previously for a series of Pd^{I} complexes incorporating tetra-aza macrocyclic ligands.⁶⁴ However, the $[\text{Pd}(\text{Me}_2[18]\text{aneN}_2\text{S}_4)]^{2+/+}$ couple occurs at a much more anodic potential than those for the tetra-aza systems. This enhanced stability of $[\text{Pd}(\text{Me}_2[18]\text{aneN}_2\text{S}_4)]^+$ is attributed to the π -acidity of the thioether S-donor atoms.

The co-ordinative versatility of $[18]\text{aneN}_2\text{S}_4$ is further exemplified by the formation of a binuclear Pd^{II} complex. Reaction of $[18]\text{aneN}_2\text{S}_4$ with two molar equivalents of PdCl_2 in refluxing $\text{CH}_3\text{CN}/\text{H}_2\text{O}$ in the absence of TIPF_6 affords the yellow complex, $[\text{Pd}_2\text{Cl}_2([18]\text{aneN}_2\text{S}_4)]^{2+}$. A single peak at 330 cm^{-1} in the

⁶⁴ A. J. Blake, R. O. Gould, T. I. Hyde, and M. Schröder, *J. Chem. Soc., Chem. Commun.*, 1987, 431; *J. Chem. Soc., Chem. Commun.*, 1987, 1730.

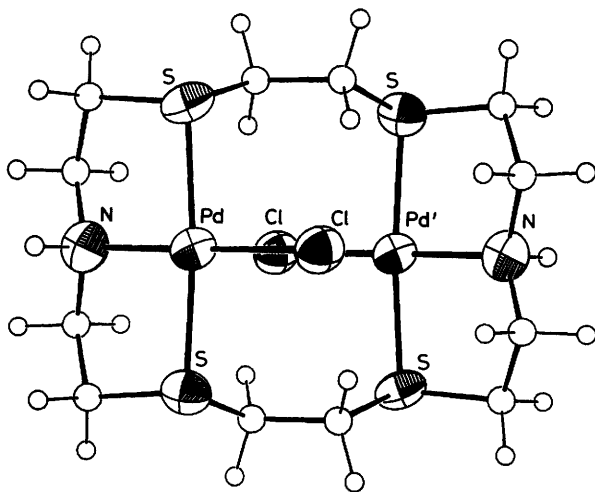


Figure 14 *Crystal structure of $[\text{Pd}_2\text{Cl}_2([\text{18}] \text{aneN}_2\text{S}_4)]^{2+}$*

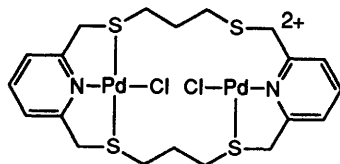


Figure 15 *Diagram of $[\text{Pd}_2\text{Cl}_2(\text{L}^2)]^{2+}$*

IR spectrum of this complex is indicative of a terminal Pd–Cl stretching vibration, $\nu(\text{Pd}-\text{Cl})$. The structure of $[\text{Pd}_2\text{Cl}_2([\text{18}] \text{aneN}_2\text{S}_4)]^{2+}$ shows a centrosymmetric cation in which each Pd^{II} centre is bound in a square plane to two S- and one N-donor of the macrocycle, $\text{Pd}-\text{S} = 2.316(4)$ and $2.317(4)$; $\text{Pd}-\text{N} = 2.049(13)$ Å, and one terminal Cl^- ligand, $\text{Pd}-\text{Cl} = 2.305(4)$ Å (Figure 14). Interestingly, the Cl^- ligands are displaced out of the least-squares NS_2Pd coordination plane by 0.0712 Å thereby reducing their interaction with the methylene chains. An intramolecular $\text{Pd} \cdots \text{Pd}$ distance of $4.196(2)$ Å confirms that the metal ions do not interact. The closest $\text{Pd} \cdots \text{Pd}$ interaction of $3.406(2)$ Å occurs between adjacent molecules related by a crystallographic 2-fold axis. Lehn and co-workers have reported a similar NS_2Cl donor set for each Pd^{II} centre in the binuclear complex $[\text{Pd}_2\text{Cl}_2(\text{L}^2)]^{2+}$ (Figure 15).⁴⁷ Treatment of PdCl_2 with the N_2S_2 -donor macrocycle, L^3 , in refluxing $\text{CH}_3\text{CN}/\text{H}_2\text{O}$ affords^{48,65} the complex cation $[\text{Pd}(\text{L}^3)]^{2+}$. Structural studies on $[\text{Pd}(\text{L}^3)](\text{PF}_6)_2$

⁶⁵ R McCrindle, G Ferguson, A J McAlees, M Parvez, and D K Stephenson, *J Chem Soc., Dalton Trans.*, 1982, 1291

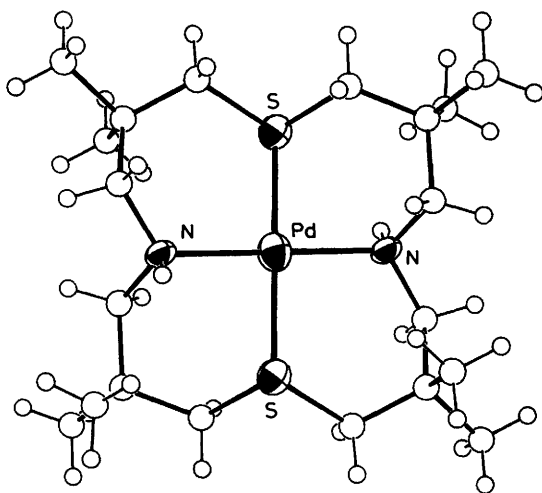


Figure 16 Crystal structure of $[\text{Pd}(\text{L}^3)]^{2+}$

show square planar co-ordination of the macrocycle to Pd^{II} via its two N- and two S-donors. The Pd^{II} ion occupies a crystallographic inversion centre, $\text{Pd-S} = 2.307(1)$, $\text{Pd-N} = 2.090(4)$ Å, with the macrocycle adopting a chair-chair conformation (Figure 16).^{48,65} The single crystal structure of the dichloride complex $[\text{Pd}(\text{L}^3)\text{Cl}_2]$ has also been reported. The structure shows two independent $[\text{Pd}(\text{L}^3)]^{2+}$ cations, each of which adopts a distorted square planar stereochemistry, $\text{Pd-S} = 2.290(5)$ – $2.297(6)$; $\text{Pd-N} = 2.05(2)$ – $2.14(2)$ Å with one apical Cl^- ion involved in a long-range, weak interaction, $\text{Pd} \cdots \text{Cl} = 3.20$ and 3.68 Å (Figure 17).^{65,66} The synthesis of the Pt^{II} analogue $[\text{Pt}(\text{L}^3)\text{Cl}_2]$ has also been reported.⁴⁸ Preparation of a Pd^{II} complex incorporating an unsaturated N_2S_2 -donor macrocyclic ligand, L^4 , has been achieved. The synthesis of $[\text{Pd}(\text{L}^4)]^{2+}$ is accomplished by the reaction of PdCl_2 with L^4 in $\text{CH}_3\text{CN}/\text{H}_2\text{O}$. The single crystal structure of this complex shows the Pd^{II} ion on an inversion centre, co-ordinated to a distorted square planar arrangement of the two N- and two S- donors of the macrocycle, $\text{Pd-S} = 2.307(1)$; $\text{Pd-N} = 2.047(4)$ Å (Figure 18).⁶⁷ The interconversion of the *meso* and *rac* diastereomers of this complex has been studied by NMR spectroscopy, giving $K(\text{rac} \rightarrow \text{meso}) = 0.36$, and $\Delta G^\ddagger = 63.3$ kJmol^{-1} at 288 K.⁶⁸

F. Platinum.—The complexes $[\text{Pt}([\text{18}] \text{aneN}_2\text{S}_4)]^{2+}$ and $[\text{Pt}(\text{Me}_2[\text{18}]-$

⁶⁶ G. Ferguson, R. McCrindle, A. J. McAlees, M. Parvez, and D. K. Stephenson, *J. Chem. Soc., Dalton Trans.*, 1983, 1865.

⁶⁷ R. McCrindle, G. Ferguson, A. J. McAlees, M. Parvez, B. L. Ruhl, D. K. Stephenson, and T. Wieckowski, *J. Chem. Soc., Dalton Trans.*, 1986, 2351.

⁶⁸ J. M. Csavas, M. R. Taylor, and K. P. Wainwright, *J. Chem. Soc., Dalton Trans.*, 1988, 2573.

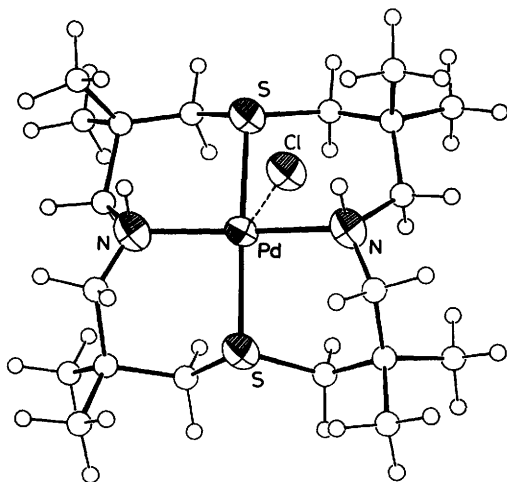


Figure 17 Crystal structure of $[\text{PdCl}_2(\text{L}^3)]$

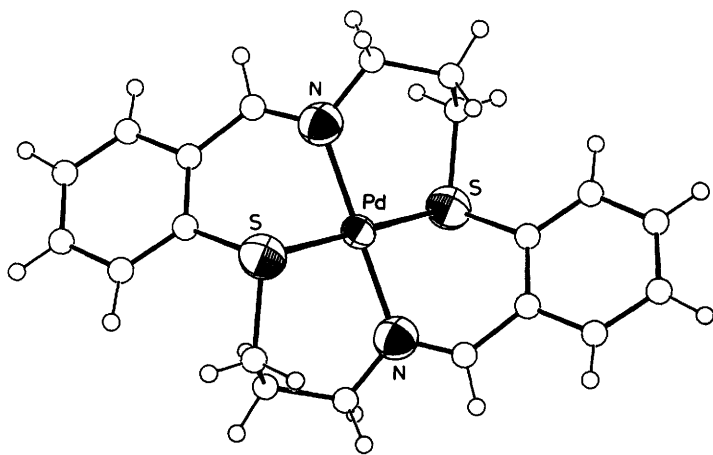


Figure 18 Crystal structure of $[\text{Pd}(\text{L}^4)]^{2+}$

$\text{aneN}_2\text{S}_4)]^{2+}$ have been synthesized by similar routes to their Pd^{II} analogues. On the basis of electrochemical and NMR data $[\text{Pt}(\text{Me}_2[18]\text{aneN}_2\text{S}_4)]^{2+}$ appears to be isostructural with $[\text{Pd}(\text{Me}_2[18]\text{aneN}_2\text{S}_4)]^{2+}$. However, $[\text{Pt}([18]\text{aneN}_2\text{S}_4)]^{2+}$ appears to be 5-co-ordinate rather than quasi-6-co-ordinate like $[\text{Pd}([18]\text{aneN}_2\text{S}_4)]^{2+}$. This assignment though must remain tentative in the absence of definitive structural evidence.

Reaction of $\text{Me}_2[18]\text{aneN}_2\text{S}_4$ with two molar equivalents of PtCl_2 in refluxing $\text{CH}_3\text{CN}/\text{H}_2\text{O}$ affords the complex cation $[\text{Pt}_2\text{Cl}_2(\text{Me}_2[18]\text{aneN}_2\text{S}_4)]^{2+}$. A single

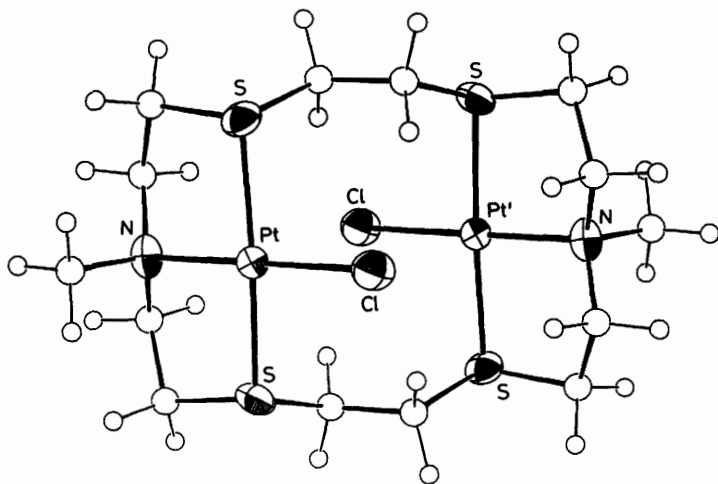


Figure 19 Crystal structure of $[\text{Pt}_2\text{Cl}_2(\text{Me}_2[18]\text{aneN}_2\text{S}_4)]^{2+}$

crystal X-ray diffraction study on this complex confirms an overall stereochemistry very similar to that of $[\text{Pd}_2\text{Cl}_2([\text{18}]\text{aneN}_2\text{S}_4)]^{2+}$ described above. The structure shows a centrosymmetric cation with square planar co-ordination to each Pt^{II} ion through two S- and one N-Me function of the macrocycle, Pt-S = 2.288(3) and 2.296(3); Pt-N = 2.048(9) Å, and one terminal Cl^- ligand, Pt-Cl = 2.296(3) Å (Figure 19). Angles at Pt^{II} deviate significantly from 90° as a consequence of the restricted bite angle of the meridional $\text{SCH}_2\text{CH}_2\text{NCH}_2\text{CH}_2\text{S}$ fragment, $\angle\text{S-Pt-N} = 87.0(3)$ and $88.0(3)^\circ$. Thus, the binuclear Pt^{II} and Pd^{II} complexes with $\text{Me}_2[18]\text{aneN}_2\text{S}_4$ and $[18]\text{aneN}_2\text{S}_4$ adopt similar stereochemistries.

G. Copper.—Macrocyclic copper complexes involving thioether co-ordination have been the focus of much attention in recent years,⁶⁹ partly due to their potential as simple models for the blue copper proteins such as plastocyanin, which involves a N_2S_2 co-ordination set through his-37, his-87, cys-84 and met-92.⁷⁰ The incorporation of mixed sulphur and nitrogen donation is an important design feature in both the metallo-enzymes and their model complexes.

⁶⁹ D. B. Rorabacher, M. M. Bernado, A. M. Q. Vande Linde, G. H. Leggett, B. C. Westerby, M. J. Martin, and L. A. Ochrymowycz, *Pure Appl. Chem.*, 1988, **60**, 501; D. B. Rorabacher, M. J. Martin, M. J. Koenigbauer, M. Malik, R. R. Schroeder, J. F. Endicott, and L. A. Ochrymowycz in 'Copper Co-ordination Chemistry: Biochemical and Inorganic Perspectives', ed. K. D. Karlin and J. Zubieta, Adenine Press, New York, 1983, p. 148.

⁷⁰ L. Rydel and J. O. Lundgren, *Nature (London)*, 1976, **261**, 344; P. M. Collman, H. C. Freeman, J. M. Guss, M. Murata, V. A. Norris, J. A. M. Ramshaw, and M. P. Venkatappa, *Nature (London)*, 1978, **272**, 319; H. C. Freeman, 'Co-ordination Chemistry', ed. J. P. Laurent, Pergamon Press, Oxford, 1981, p. 29.

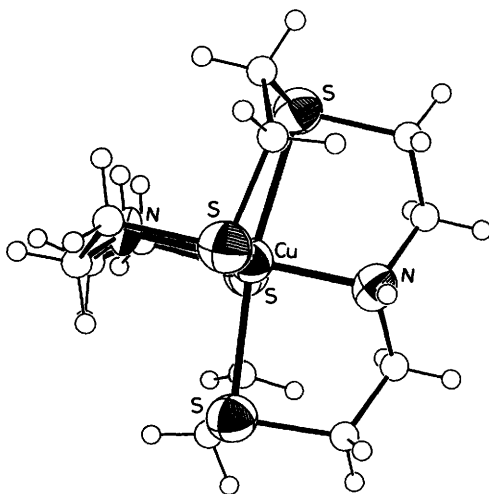


Figure 20 Crystal structure of $[\text{Cu}([\text{18}]\text{aneN}_2\text{S}_4)]^{2+}$

Treatment of $\text{Cu}(\text{NO}_3)_2$ with one molar equivalent of $[\text{18}]\text{aneN}_2\text{S}_4$ in refluxing $\text{EtOH}/\text{H}_2\text{O}$ affords the bright green complex $[\text{Cu}[\text{18}]\text{aneN}_2\text{S}_4]^{2+}$. The single crystal *X*-ray structure of this complex-cation shows an unusual tetragonally compressed stereochemistry in which the Cu^{II} ion is bound to all six donor atoms in a *rac* configuration (Figure 20).¹⁴ The tetragonal compression occurs along the $\text{N}-\text{Cu}-\text{N}$ axis, $\text{Cu}-\text{N} = 2.007(13)$ and $2.036(12)$ Å, and the conformational rigidity of the macrocycle results in the four equatorial S -donors being pulled away from the Cu centre to give very long $\text{Cu}-\text{S}$ distances, $\text{Cu}-\text{S} = 2.577(5)$, $2.487(5)$, $2.528(5)$, and $2.578(5)$ Å. In contrast, *meso* $[\text{Cu}([\text{18}]\text{aneS}_6)]^{2+}$ exhibits a tetragonally elongated stereochemistry, $\text{Cu}-\text{S} = 2.323(1)$, $2.402(1)$, and $2.635(1)$ Å,³⁰ while $[\text{Cu}([\text{19}]\text{aneS}_3)_2]^{2+}$ shows an octahedral geometry with each tridentate macrocycle binding facially, $\text{Cu}-\text{S} = 2.419(3)$, $2.426(3)$, and $2.459(3)$ Å.³⁸ Interestingly, Hancock and co-workers have reported that the complex $[\text{Cu}([\text{9}]\text{aneN}_2\text{S}_2)]^{2+}$ shows an exceptionally long $\text{Cu}-\text{S}$ bond length of $2.707(1)$, with $\text{Cu}-\text{N} = 2.027(3)$ and $2.067(3)$ Å.⁷¹ This allows the co-ordinated macrocycles to adopt a $[\text{234}]$ conformation which reduces unfavourable non-bonding interactions and thereby minimizes strain energy.

Treatment of $\text{Cu}(\text{NO}_3)_2$ with one molar equivalent of $\text{Me}_2[\text{18}]\text{aneN}_2\text{S}_4$ in refluxing $\text{EtOH}/\text{H}_2\text{O}$ affords a green solution of $[\text{Cu}(\text{Me}_2[\text{18}]\text{aneN}_2\text{S}_4)]^{2+}$. The single crystal *X*-ray structure of this complex-cation shows the Cu^{II} ion coordinated *via* all six macrocyclic donor atoms in a distorted octahedral environment, $\text{Cu}-\text{S} = 2.496(5)$, $\text{Cu}-\text{N} = 2.191(17)$ Å with the macrocyclic ring adopting the *meso* configuration (Figure 21).¹⁴ Importantly therefore, on going

⁷¹ J C A Boeyens, S M Dobson, and R D Hancock, *Inorg Chem*, 1985, 24, 3073

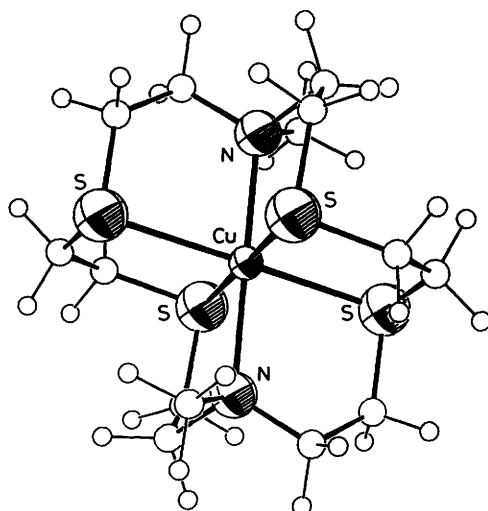


Figure 21 Crystal structure of $[\text{Cu}(\text{Me}_2[18]\text{aneN}_2\text{S}_4)]^{2+}$

Table 3 Redox properties for octahedral copper macrocyclic complexes

Complex	$E_4(\text{V}) \text{Cu}^{\text{III}}$	Ref.
$[\text{Cu}([18]\text{aneS}_6)]^{2+}$	+0.24	30
$[\text{Cu}([9]\text{aneS}_3)_2]^{2+}$	+0.12	30
$[\text{Cu}(\text{Me}_2[18]\text{aneN}_2\text{S}_4)]^{2+}$	+0.06	14
$[\text{Cu}([18]\text{aneN}_2\text{S}_4)]^{2+}$	-0.31	14
$[\text{Cu}([9]\text{aneN}_3)_2]^{2+}$	-1.41 (irreversible)	72

from $[\text{Cu}([18]\text{aneN}_2\text{S}_4)]^{2+}$ to $[\text{Cu}(\text{Me}_2[18]\text{aneN}_2\text{S}_4)]^{2+}$ the configuration changes from *rac* to *meso* and the axial Cu–N distances increase with a concomitant decrease in the Cu–S distances. The effect of the marked stereochemical difference between $[\text{Cu}([18]\text{aneN}_2\text{S}_4)]^{2+}$ and $[\text{Cu}(\text{Me}[18]\text{aneN}_2\text{S}_4)]^{2+}$ is also apparent in the electrochemical properties of these complexes.

The cyclic voltammogram of $[\text{Cu}([18]\text{aneN}_2\text{S}_4)]^{2+}$ shows a reversible Cu^{III} redox couple at $E_3 = -0.31 \text{ V vs Fc/Fc}^+$. In contrast, the di-*N*-methylated complex, $[\text{Cu}(\text{Me}_2[18]\text{aneN}_2\text{S}_4)]^{2+}$, exhibits a reversible Cu^{II} couple at a significantly more anodic potential, $E_4 = +0.06 \text{ V vs Fc/Fc}^+$. This difference in reduction potential arises from the much greater interaction of the Cu^{II} ion with the soft thioether S-donors in $[\text{Cu}(\text{Me}_2[18]\text{aneN}_2\text{S}_4)]^{2+}$, thus providing greater stability of the low-valent Cu^{I} species. The hexathia Cu^{II} analogues $[\text{Cu}([18]\text{aneS}_6)]^{2+}$ and $[\text{Cu}([9]\text{aneS}_3)_2]^{2+}$ both show reversible Cu^{III} couples at

⁷² A. D. Beveridge, A. J. Lavery, M. D. Walkinshaw, and M. Schröder, *J. Chem. Soc., Dalton Trans.*, 1987, 373; P. Chaudhuri, K. Oder, K. Wieghardt, J. Weiss, J. Reedijk, W. Hinrichs, J. Wood, A. Ozarowski, H. Stratenmeier, and D. Reinen, *Inorg. Chem.*, 1986, **25**, 2951.

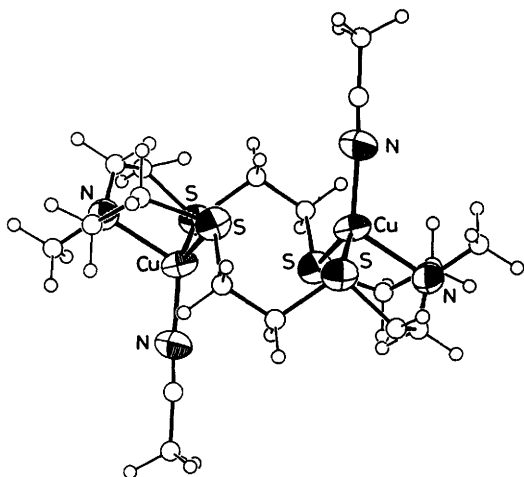


Figure 22 Crystal structure of $[\text{Cu}_2(\text{Me}_2[18]\text{aneN}_2\text{S}_4)(\text{NCCH}_3)_2]^{2+}$

highly positive potentials, reflecting the net π -acidity of six thioether donors³⁰ Redox properties of some copper complexes are given in Table 3

Preparation of the air-stable binuclear Cu^{I} complex $[\text{Cu}(\text{Me}_2[18]\text{aneN}_2\text{S}_4)(\text{NCMe})_2]^{2+}$ can be achieved by reaction of $\text{Me}_2[18]\text{aneN}_2\text{S}_4$ with two molar equivalents of $[\text{Cu}(\text{NCCH}_3)_4]^+$ in refluxing CH_3CN ¹⁴ A single crystal structure determination of this complex reveals a centrosymmetric structure with each Cu^{I} centre bound tetrahedrally to two S- and one N-donor of the macrocycle, $\text{Cu-S} = 2.317(4), 2.286(4)$, $\text{Cu-N} = 2.165(7)\text{\AA}$, and one NCMe molecule, $\text{Cu-N} = 1.924(9)\text{\AA}$ (Figure 22)¹⁴ The intramolecular $\text{Cu}\cdots\text{Cu}$ separation is $4.283(2)\text{\AA}$, with each Cu^{I} ion bound by an N_2S_2 donor set similar to that found in Type 1 copper proteins⁷⁰ A very similar structure has been determined for $[\text{Cu}_2([\text{18}\text{aneS}_6)(\text{NCMe})_2]^{2+}$, which shows NS_3 co-ordination to each Cu^{I} centre⁷³

H. Silver.—Reaction of AgNO_3 with one molar equivalent of $[18]\text{aneN}_2\text{S}_4$ in refluxing $\text{CH}_3\text{OH}/\text{H}_2\text{O}$ yields the light-sensitive Ag^{I} complex $[\text{Ag}([18]\text{aneN}_2\text{S}_4)]^+$, the structure of which shows a highly distorted octahedral stereochemistry The Ag^{I} ion is bound to four thioether S-donors, $\text{Ag-S} = 2.630(4), 2.664(4), 2.719(4), \text{and } 2.774(4)\text{\AA}$, and two apical N-donors, $\text{Ag-N} = 2.553(10)$ and $2.817(15)\text{\AA}$ (Figure 23) The complex, although extremely irregular, can be regarded as adopting a *rac* configuration There is a severe tetrahedral distortion of the four S-donors out of the least-squares S_4 co-ordination plane The Ag^{I} centre may alternatively be regarded as five-co-ordinate to an NS_4 donor set with an additional long-range interaction of the second N-donor The structure of

⁷³ R. O. Gould, A. J. Lavery and M. Schroder *J. Chem. Soc. Chem. Commun.* 1985, 1492

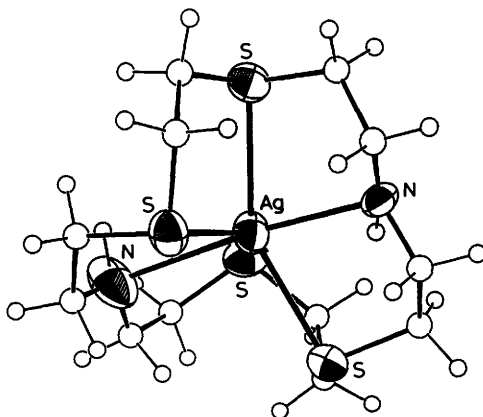


Figure 23 Crystal structure of $[\text{Ag}([\text{18}]\text{aneN}_2\text{S}_4)]^+$

$[\text{Ag}([\text{18}]\text{aneN}_2\text{S}_4)]^+$ contrasts with that of the related homoleptic hexathia macrocyclic complexes, $[\text{Ag}([\text{9}]\text{aneS}_3)_2]^+$ and $[\text{Ag}([\text{18}]\text{aneS}_6)]^+$. These structures each show a centrosymmetric $[\text{AgS}_6]^+$ ionophore in a tetragonally distorted stereochemistry, $\text{Ag-S} = 2.697(5)$ and $2.753(4)$ Å for $[\text{Ag}([\text{9}]\text{aneS}_3)_2]^+$,⁷⁴ and $\text{Ag-S} = 2.6665(12)$ and $2.7813(10)$ Å for $[\text{Ag}([\text{18}]\text{aneS}_6)]^+$.³⁴

The complex $[\text{Ag}(\text{Me}_2[\text{18}]\text{aneN}_2\text{S}_4)]^+$ can be prepared by reaction of AgNO_3 with $\text{Me}_2[\text{18}]\text{aneN}_2\text{S}_4$ in refluxing $\text{MeOH}/\text{H}_2\text{O}$. The crystal structure of this light-sensitive complex was disordered showing two different macrocyclic configurations. The major component [70.2(8)%] adopts an unusual kite-based pyramidal geometry at Ag^1 via co-ordination to a near planar arrangement of four S-donors, $\text{Ag-S} = 2.583(4)$, $2.819(3)$, $2.663(4)$, and $2.673(4)$ Å, with one N-donor bound apically, $\text{Ag-N} = 2.517(11)$ Å. The second N-donor is directed away from the metal ion and does not interact with it, $\text{Ag} \cdots \text{N}' = 3.684(11)$ Å [Figure 24(a)]. Importantly, the complex shows a *meso*-like configuration similar to the Cu analogue, $[\text{Cu}(\text{Me}_2[\text{18}]\text{aneN}_2\text{S}_4)]^{2+}$. The structure of the minor [29.2(8)%] component [Figure 24(b)] differs from that of the major component only in the configuration around the second N-donor atom (N''). In this case, both N-donors are directed towards, and co-ordinated to the Ag ion, $\text{Ag-N}'' = 2.778(10)$ Å, giving a distorted octahedral stereochemistry, in a genuine *meso*-configuration.

The synthesis of the related N_4S_2 -donor macrocycles $[\text{18}]\text{aneN}_4\text{S}_2$ and $\text{Me}_4[\text{18}]\text{aneN}_4\text{S}_2$ has been reported.⁷⁵ These macrocycles readily bind Ag^1 to give $[\text{Ag}([\text{18}]\text{aneN}_4\text{S}_2)]^+$ and $[\text{Ag}(\text{Me}_4[\text{18}]\text{aneN}_4\text{S}_2)]^+$ respectively. The structure of $[\text{Ag}([\text{18}]\text{aneN}_4\text{S}_2)]^+$ shows (Figure 25), distorted octahedral co-ordina-

⁷⁴ H. J. Küppers, K. Wiegardt, Y. H. Tsay, C. Krüger, B. Nuber, and J. Weiss, *Angew. Chem.*, 1987, **99**, 583; *Angew. Chem., Int. Ed. Engl.*, 1987, **27**, 575; J. Clarkson, R. Yagbasan, P. J. Blower, S. C. Rawle, and S. R. Cooper, *J. Chem. Soc., Chem. Commun.*, 1987, 959.

⁷⁵ A. S. Craig, R. Katakay, D. Parker, H. Adams, N. Bailey, and H. Schneider, *J. Chem. Soc., Chem Commun.*, 1989, 1870.

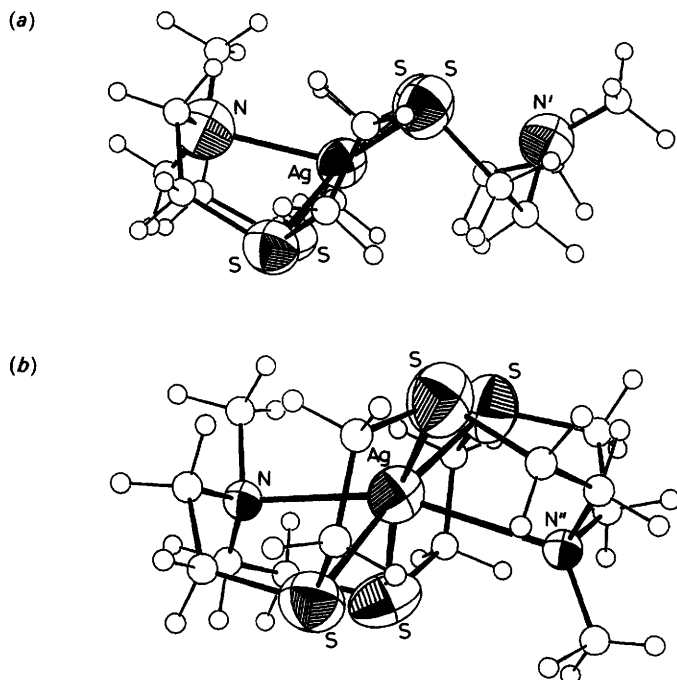


Figure 24 Crystal structure of $[\text{Ag}(\text{Me}_2[18]\text{aneN}_2\text{S}_4)]^+$ showing (a) NS_4 co-ordination in major component (b) N_2S_4 co-ordination in minor component

tion of the macrocycle to Ag^{I} via four N-donors, $\text{Ag}-\text{N} = 2.553(11)$ and $2.589(10)$ Å, and two S-donors, $\text{Ag}-\text{S} = 2.658(5)$ Å, to give a *meso*-isomer. The preparation of $[\text{Ag}(\text{L}^3)(\text{OCOCH}_3)]$ has also been reported. The crystal structure of this species shows Ag^{I} bound through the four macrocyclic donors and one acetate ligand, generating a square-pyramidal stereochemistry, $\text{Ag}-\text{S} = 2.589(1)$; $\text{Ag}-\text{N} = 2.481(2)$ and $2.430(2)$; $\text{Ag}-\text{O} = 2.686(2)$ Å (Figure 26). The four six-membered chelate rings involving the macrocycle have twist-boat conformations with mutually *cis* NH groups.⁷⁶

Cyclic voltammetry of $[\text{Ag}([18]\text{aneN}_2\text{S}_4)]^+$ shows an oxidation at $E_{\frac{1}{2}} = +0.65$ V and a quasi-reversible reduction $E_{\frac{1}{2}} = -0.74$ V vs Fc/Fc^+ assigned to $\text{Ag}^{\text{I/III}}$ and $\text{Ag}^{\text{I/0}}$ couples respectively. The complexes $[\text{Ag}([9]\text{aneS}_3)_2]^+$ and $[\text{Ag}([18]\text{aneS}_6)]^+$ show $\text{Ag}^{\text{I/III}}$ couples at $E_{\frac{1}{2}} = +0.75$ and $E_{\text{pa}} = +1.00$ V respectively and $\text{Ag}^{\text{I/0}}$ couples at $E_{\text{pc}} = -0.57$ and $E_{\frac{1}{2}} = -0.42$ V vs Fc/Fc^+ respectively. The potentials for these redox processes are consistent with the differences expected for S_6 - versus N_2S_4 -donor sets.^{34,74} Controlled potential oxidation of $[\text{Ag}([18]\text{aneN}_2\text{S}_4)]^+$ affords an unstable blue Ag^{II} species. The

⁷⁶ G. Ferguson, R. McCrindle, and M. Parvez, *Acta Crystallogr., Sect. C*, 1984, **40**, 354.

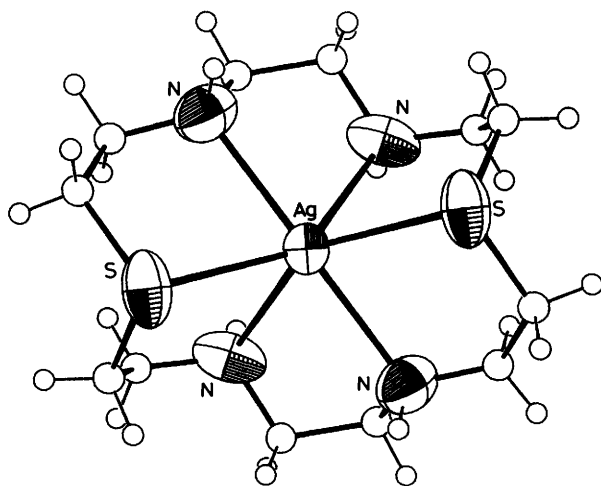


Figure 25 Crystal structure of $[\text{Ag}([\text{18}]\text{aneN}_4\text{S}_2)]^+$

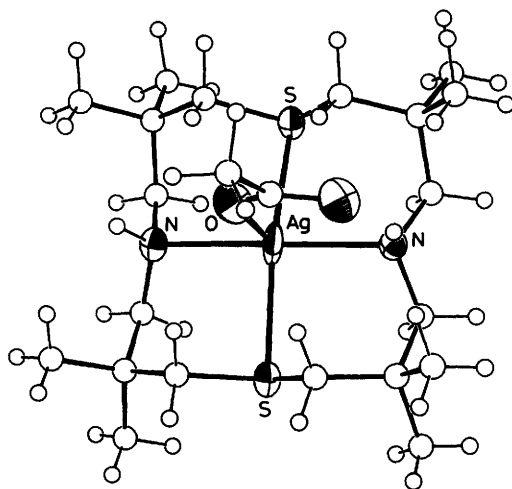


Figure 26 Crystal structure of $[\text{Ag}(\text{L}^3)(\text{OAc})]$

stabilization of the related Ag^{II} complexes $[\text{Ag}([\text{9}]\text{aneS}_3)_2]^{2+}$ and $[\text{Ag}([\text{18}]\text{aneS}_6)]^{2+}$ by highly acidic media has been reported.³⁴ Attempts to stabilize $[\text{Ag}([\text{18}]\text{aneN}_2\text{S}_4)]^{2+}$ under the same conditions does lead to some enhanced stability of the complex cation although decomposition, presumably *via* protonation of the N-donors, occurs over a period of minutes.

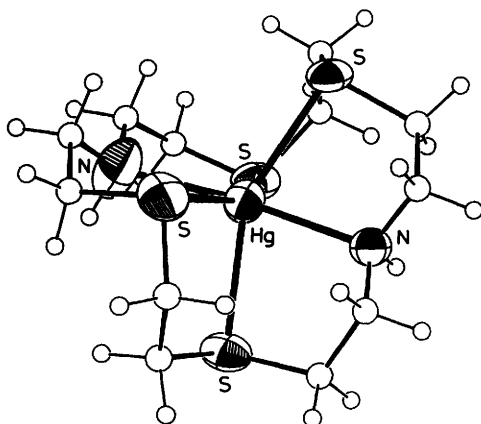


Figure 27 Crystal structure of $[\text{Hg}([\text{18}]\text{aneN}_2\text{S}_4)]^{2+}$

I. Mercury.—The synthesis of the octahedral Hg^{II} complex $[\text{Hg}([\text{18}]\text{aneN}_2\text{S}_4)]^{2+}$ is achieved by the reaction of HgSO_4 with $[\text{18}]\text{aneN}_2\text{S}_4$ in refluxing $\text{CH}_3\text{OH}/\text{H}_2\text{O}$. Like its Ag^{I} analogue $[\text{Ag}([\text{18}]\text{aneN}_2\text{S}_4)]^+$, $[\text{Hg}([\text{18}]\text{aneN}_2\text{S}_4)]^{2+}$ exhibits a severely distorted octahedral stereochemistry in the crystal, with Hg^{II} bound to all six macrocyclic donor atoms, $\text{Hg-S} = 2.639(5)$, $2.655(5)$, $2.735(4)$, and $2.751(4)$ Å; $\text{Hg-N} = 2.472(17)$ and $2.473(11)$ Å (Figure 27). There is a large tetrahedral distortion of the thioether S-donors out of the least-squares S_4 co-ordination plane, presumably a consequence of the large Hg^{II} ion radius. This distortion, however, is not as great as for $[\text{Ag}([\text{18}]\text{aneN}_2\text{S}_4)]^+$. The structure of $[\text{Hg}([\text{9}]\text{aneS}_3)_2]^{2+}$ differs considerably from that of $[\text{Hg}([\text{18}]\text{aneN}_2\text{S}_4)]^{2+}$; $[\text{Hg}([\text{9}]\text{aneS}_3)_2]^{2+}$ shows a centrosymmetric cation with a significant tetragonal compression, $\text{Hg-S} = 2.638(3)$, $2.712(3)$, and $2.728(3)$ Å.⁷⁷ $[\text{Hg}(\text{L}^3)\text{Cl}_2]$ can be prepared by treatment of HgCl_2 with L^3 in refluxing EtOH .⁴⁸

4 Conclusions

The Fe^{II} , Co^{III} , Ni^{II} , Cu^{II} , Ag^{I} , Hg^{II} , Rh^{III} , and by implication, Co^{II} complexes of $[\text{18}]\text{aneN}_2\text{S}_4$ all show octahedral *rac* configurations with *anti* C–C–N–C linkages. This contrasts with the corresponding $[\text{18}]\text{aneS}_6$ complexes which all show *meso* configurations with no *anti* C–C–S–C linkages. In general, the complexes $[\text{M}([\text{18}]\text{aneN}_2\text{S}_4)]^{x+}$ which we have studied participate in substantial H-bonding through the N–H functions, giving well ordered crystal structures. In contrast, replacement of N–H by N–Me functions gives complexes which are unable to H-bond, and which often exhibit disorder around the aza-functions. The degree of distortion at the metal co-ordination sphere of the complexes $[\text{M}([\text{18}]\text{aneN}_2\text{S}_4)]^{x+}$ can be assessed by considering the degree of tetrahedral

⁷⁷ A J Blake, A J Holder, T I Hyde, G Reid, and M Schroder, *Polyhedron*, 1989, 8, 2041

Table 4 Tetrahedral distortion in octahedral complexes $\text{rac-}[\text{M}([\text{18}] \text{aneN}_2\text{S}_4)]^{x+}$

<i>M</i>	Ionic radius of <i>M</i> (Å)	Deviation of <i>S</i> out of least-squares <i>S</i> ₄ -donor plane (Å)			
		S(1)	S(4)	S(10)	S(13)
Co ^{III}	0.545	+0.120	-0.120	-0.121	+0.120
Fe ^{II}	0.61	+0.137	-0.137	-0.139	+0.139
Rh ^{III}	0.665	+0.174	-0.175	-0.175	+0.176
Ni ^{II}	0.69	+0.227	-0.224	-0.228	+0.225
Cu ^{II}	0.73	+0.230	-0.228	-0.231	+0.232
Hg ^{II}	1.02	+0.658	-0.670	-0.652	+0.664
Ag ^I	1.15	+0.792	-0.779	-0.782	+0.769

S(1) *trans* to S(13); S(4) *trans* to S(10); + = above the plane; - = below the plane.

distortion of each S-donor from the least-squares *S*₄ plane. Table 4 summarizes this structural data for each complex. There appears to be a direct correlation between the ionic radius of the complexed metal ion and the degree of tetrahedral distortion of the *S*₄-donor atoms. Thus Co^{III}, which has the smallest ionic radius (0.545 Å), results in the smallest distortion of the macrocyclic donors. The largest tetrahedral distortion is for Ag^I, the metal ion with the largest ionic radius (1.15 Å). Thus, a mechanism based on hole-size factors is operating, wherein [18]aneN₂S₄ distorts to accommodate the appropriate metal ion. We are currently investigating the co-ordinative properties of [18]aneN₂S₄ with larger metal nuclei such as Au^I (ionic radius 1.37 Å). We have recently reported the synthesis of [Au([9]aneS₃)₂]⁺ and [Au([18]aneS₆)]⁺ and have confirmed that the former species adopts a distorted tetrahedral stereochemistry in the solid state.⁷⁸ In principle, therefore, the structure of [Au([18]aneN₂S₄)]⁺ should involve greater distortion towards a fully tetrahedral geometry compared to the corresponding Ag^I species.

Another feature of [18]aneN₂S₄ co-ordination chemistry is the requirement that the two N-donors bind apically at mutually *trans* sites of the octahedral metal centre. Since simple ionic radius considerations suggest that M–N distances should be shorter than M–S(thioether) distances, the N-donors of [18]aneN₂S₄ have therefore to make a closer approach to the metal ion than do the S-donors: this limits the approach of the S-donors to the metal ion. Thus, octahedral complexes of [18]aneN₂S₄ tend to show long M–S bond lengths compared to the corresponding *meso* [M([18]aneS₆)]^{x+} and [M([9]aneS₃)₂]^{x+} complexes. For [Cu([18]aneN₂S₄)]²⁺, the Cu–S distances are further elongated by Jahn–Teller distortion imposed by the *d*⁹ metal ion.¹³ The constriction of M–S bonds in *meso* [M([18]aneS₆)]²⁺ complexes has been documented.⁴

The complexes [M([18]aneN₂S₄)]^{x+} often show oxidative and reductive couples which are more cathodic than the corresponding [M([9]aneS₃)₂]²⁺ and [M([18]aneS₆)]²⁺ complexes. This is a reflection of S₆ *vs* N₂S₄ co-ordination.

⁷⁸ A. J. Blake, R. O. Gould, J. A. Greig, A. J. Holder, T. I. Hyde, and M. Schroder, *J. Chem. Soc., Chem Commun.*, 1989, 876; A. J. Blake, J. A. Greig, A. J. Holder, T. I. Hyde, A. Taylor, and M. Schröder, *Angew. Chem.*, 1990, **102**, 203; *Angew. Chem., Int. Ed. Engl.*, 1990, **29**, 197.

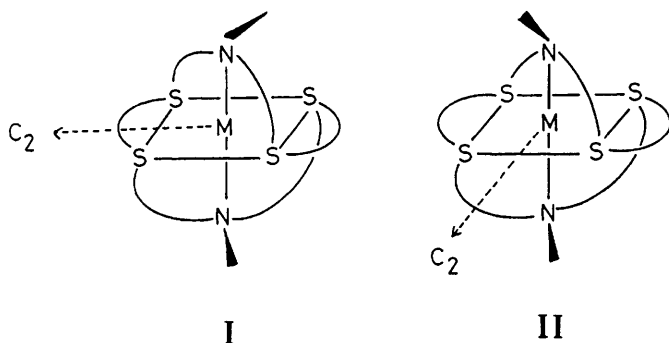


Figure 28 Diastereoisomers of $rac\text{-}[M([18]aneN_2S_4)]^{x+}$

The ligands $[18]aneN_2S_4$ and $Me_2[18]aneN_2S_4$ clearly show very different coordinative properties. Whereas the *rac* isomer predominates for the octahedral complexes of $[18]aneN_2S_4$, all the octahedral complexes $[M(Me_2[18]aneN_2S_4)]^{2+}$ which we have studied to date can be assigned as *meso* isomers on the basis of structural studies and/or redox and spectroscopic data. A principal reason for this profound difference in co-ordinative properties (and consequently in complex reactivity) is that the N-Me function is sterically more demanding than its N-H parent. An 18-membered ring incorporating methylated N-donors will minimize ring strain and alleviate the steric interactions between methylene and methyl protons by adopting a *meso* configuration for a mononuclear octahedral complex. As a result, M-N bond lengths are longer (and M-S bond lengths necessarily shorter) in $[M(Me_2[18]aneN_2S_4)]^{2+}$ than in $[M([18]aneN_2S_4)]^{2+}$; these differences are reflected in the redox properties of these complexes. These structural factors are not relevant for dimeric species such as $[Pd_2Cl_2([18]aneN_2S_4)]^{2+}$ since the macrocycle can readily span two metal ions meridionally.

The complexes which are anomalous are of course the d^8 Pd^{II} and Pt^{II} species.⁶⁰ For these metal centres a fundamental mis-match exists between the potentially octahedral ligands and the square planar metal centres. This results in complexes where a compromise between ligation and stereochemistry is achieved.

Finally, a further point of interest in complexes of the type $rac\text{-}[M([18]aneN_2S_4)]^{x+}$ is the potential presence of two diastereoisomers, (I) and (II) (Figure 28). Searle, Hay, and co-workers have recognized the non-equivalence of these isomers in the complex cation $rac\text{-}[Co([18]aneN_6)]^{3+}$, and have studied the interconversion of *rac* and *meso* configurations for this species.⁷⁹ The ^{13}C NMR spectra of $rac\text{-}[M([18]aneN_2S_4)]^{3+}$ ($M = Fe, Rh$) in CD_3CN each show *two* sets of six resonances (in an approximately 2:1 ratio) assigned to the C-

⁷⁹ R W Hay, B Jeragh, S F Lincoln, and G H Searle, *Inorg Nucl Chem Lett*, 1978, 14, 435, Y Yoshikawa, *Chem Lett*, 1978, 109, G H Searle and M E Angley, *Inorg Chim Acta*, 1981, 49, 185
We thank Professor Hay for communicating unpublished results to us

centres of the co-ordinated crown. Since the *meso* isomer would be expected to show only three separate resonances for the C-centres of co-ordinated [18]aneN₂S₄, we assign the observed solution spectrum to a mixture of the two non-equivalent *rac* isomers, (I) and (II). Significantly, the crystal structures of *rac*-[M([18]aneN₂S₄)]³⁺ (M = Fe, Figure 4; M = Rh, Figure 6) show the complexes to adopt configuration (I) suggesting that this diastereoisomer has crystallized preferentially.

Acknowledgements. We are very grateful to Dr. Alexander J. Blake and Dr. Robert O. Gould for their considerable help in structure determinations and developing disorder models for many of the compounds described herein. In addition we wish to thank Dr. Nigel Atkinson, Dr. Michael G. B. Drew, and Dr. Aidan J. Lavery for collaboration on aspects of the first row metal complexes described. We gratefully acknowledge SERC for support, and Johnson Matthey Plc for loans of precious metals.